



Innate Immune Responses of Bat and Human Cells to Filoviruses: Commonalities and Distinctions

Ivan V. Kuzmin,^{a,b} Toni M. Schwarz,^c Philipp A. Ilinykh,^{a,b} Ingo Jordan,^{d*} Thomas G. Ksiazek,^{a,b,e} Ravi Sachidanandam,^f Christopher F. Basler,^{c*} Alexander Bukreyev^{a,b,e}

Department of Pathology, The University of Texas Medical Branch, Galveston, Texas, USA^a; Galveston National Laboratory, The University of Texas Medical Branch, Galveston, Texas, USA^b; Department of Microbiology, Icahn School of Medicine at Mount Sinai, New York, New York, USA^c; ProBioGen AG, Berlin, Germany^d; Department Microbiology & Immunology, The University of Texas Medical Branch, Galveston, Texas, USA^e; Department of Oncological Sciences, Icahn School of Medicine at Mount Sinai, New York, New York, USA^f

ABSTRACT Marburg (MARV) and Ebola (EBOV) viruses are zoonotic pathogens that cause severe hemorrhagic fever in humans. The natural reservoir of MARV is the Egyptian rousette bat (*Rousettus aegyptiacus*); that of EBOV is unknown but believed to be another bat species. The Egyptian rousette develops subclinical productive infection with MARV but is refractory to EBOV. Interaction of filoviruses with hosts is greatly affected by the viral interferon (IFN)-inhibiting domains (IID). Our study was aimed at characterization of innate immune responses to filoviruses and the role of filovirus IID in bat and human cells. The study demonstrated that EBOV and MARV replicate to similar levels in all tested cell lines, indicating that permissiveness for EBOV at cell and organism levels do not necessarily correlate. Filoviruses, particularly MARV, induced a potent innate immune response in rousette cells, which was generally stronger than that in human cells. Both EBOV VP35 and VP24 IID were found to suppress the innate immune response in rousette cells, but only VP35 IID appeared to promote virus replication. Along with IFN- α and IFN- β , IFN- γ was demonstrated to control filovirus infection in bat cells but not in human cells, suggesting host species specificity of the antiviral effect. The antiviral effects of bat IFNs appeared not to correlate with induction of IFN-stimulated genes 54 and 56, which were detected in human cells ectopically expressing bat IFN- α and IFN- β . As bat IFN- γ induced the type I IFN pathway, its antiviral effect is likely to be partially induced via cross talk.

IMPORTANCE Bats serve as reservoirs for multiple emerging viruses, including filoviruses, henipaviruses, lyssaviruses, and zoonotic coronaviruses. Although there is no evidence for symptomatic disease caused by either Marburg or Ebola viruses in bats, spillover of these viruses into human populations causes deadly outbreaks. The reason for the lack of symptomatic disease in bats infected with filoviruses remains unknown. The outcome of a virus-host interaction depends on the ability of the host immune system to suppress viral replication and the ability of a virus to counteract the host defenses. Our study is a comparative analysis of the host innate immune response to either MARV or EBOV infection in bat and human cells and the role of viral interferon-inhibiting domains in the host innate immune responses. The data are useful for understanding the interactions of filoviruses with natural and accidental hosts and for identification of factors that influence filovirus evolution.

KEYWORDS accidental host, bat, Ebola virus, Marburg virus, immune evasion, interferon-inhibiting domain, interferons, natural host

Received 22 December 2016 Accepted 17 January 2017

Accepted manuscript posted online 25 January 2017

Citation Kuzmin IV, Schwarz TM, Ilinykh PA, Jordan I, Ksiazek TG, Sachidanandam R, Basler CF, Bukreyev A. 2017. Innate immune responses of bat and human cells to filoviruses: commonalities and distinctions. *J Virol* 91:e02471-16. <https://doi.org/10.1128/JVI.02471-16>.

Editor Douglas S. Lyles, Wake Forest University

Copyright © 2017 American Society for Microbiology. All Rights Reserved.

Address correspondence to Alexander Bukreyev, alexander.bukreyev@utmb.edu.

* Present address: Christopher F. Basler, Center for Microbial Pathogenesis, Institute for Biomedical Sciences, Georgia Research Alliance, Eminent Scholar in Virology, Georgia State University, Atlanta, Georgia, USA; Ingo Jordan, CureVac AG, Tübingen, Germany.

Ebola (EBOV) and Marburg (MARV) viruses (family *Filoviridae*, order *Mononegavirales*) cause severe hemorrhagic fever with high fatality in human and nonhuman primates. The pathogenic effects of filovirus infections in primates are multiple and complex. Infection results in high levels of uncontrolled virus replication, excessive cytokine production, and release of mediators that contribute to tissue damage, vascular leakage, and bleeding (1). The pathology is exacerbated by the ability of filoviruses to antagonize the innate immune response (2–4).

Type I interferons (IFNs), which include IFN- α and IFN- β , are critical components of the innate immune system. They are secreted by cells of many different types as the primary response to infection (5, 6). Type II IFN, also known as IFN- γ , is an important activator of macrophages and inducer of class I major histocompatibility complex molecule expression (7). Although IFN- γ utilizes its own receptors and signaling pathways (8), it may also induce type I IFN responses via cross talk (9). Interleukin-29 (IL-29), together with IL-28A and IL-28B, constitute type III IFNs, or IFN- λ , which in humans are secreted by multiple types of cells and especially by respiratory epithelial cells (10–12). Expression of IFNs is induced by activation of pattern recognition receptors (PRR) in infected cells. When expressed and secreted, IFNs trigger the JAK-STAT signaling cascade, which upregulates multiple genes that induce an antiviral state in the infected and neighboring uninfected cells (6, 13).

Filovirus genomes encode seven structural proteins, in the order NP-VP35-VP40-GP-VP30-VP24-L (14). Several of these were found to contain IFN-inhibiting domains (IID). Studies with human or nonhuman primate cells demonstrated that EBOV VP35 IID plays a critical role in suppression of the production of type I IFNs by counteracting RIG-I-like receptor signaling (reviewed in reference 4). Point mutations in VP35 IID resulted in an increase of a type I IFN response, the maturation of human dendritic cells that is normally blocked by EBOV infection, and the consequential activation of T lymphocytes, B lymphocytes, and NK cells. This increased immune response leads to an attenuation of the EBOV VP35 mutant *in vitro* and in animal models of filovirus infection (15–20).

The EBOV VP24 IID antagonizes type I interferon signaling by blocking tyrosine-phosphorylated STAT1 (PY-STAT1) transport into the nucleus. Interferon signaling leads to the phosphorylation and dimerization of STAT1 and STAT2 and their subsequent nuclear import via the NPI-1 subfamily of karyopherins (4). Nuclear import of PY-STAT1 allows for the transcriptional induction of interferon-stimulated genes (ISGs). VP24 competes for an overlapping binding site with PY-STAT1 on the NPI-1 subfamily of karyopherin α (KPN α) transporter proteins, thereby ablating the antiviral response. A K142A mutation in the EBOV VP24 IID decreases its affinity for KPN α 5 and increases the innate response to infection in dendritic cells and greater induction of cell-mediated response, although these effects are not nearly as profound as the effects of infection with the VP35 IID mutant virus (15, 20, 21). No immunosuppressive function has been documented in MARV VP24 to date. Instead, MARV VP40 protein inhibits tyrosine phosphorylation events that are essential for IFN signaling in cells, presumably by blocking Jak1 kinase function (22).

Bats (order Chiroptera) have been recognized as reservoirs of several important zoonotic viruses, including henipaviruses, lyssaviruses, and Middle East respiratory syndrome (MERS) and severe acute respiratory syndrome (SARS) coronaviruses (23). They have also been increasingly implicated as the reservoir hosts of filoviruses (24–27). MARV has been repeatedly isolated from Egyptian rousette bats (*Rousettus aegyptiacus*) in Uganda (25, 26). It is generally assumed that the natural reservoir hosts of filoviruses would not develop a severe disease with high fatality like that seen in primates. Consistent with this expectation, experimental infection of three bat species with EBOV resulted in a subclinical manifestation with transient viremia, a limited virus replication in blood and selected tissues, and shedding with saliva and feces (28, 29). Similar results were documented with the Egyptian rousette bats infected with MARV, where replication occurred but overt signs of illness were absent. Notably, this same bat species was demonstrated to be refractory to experimental infection with EBOV (30–32).

TABLE 1 Sequence identity values between innate immune genes of Egyptian rousette generated in this study and other mammalian counterparts

Gene (mRNA)	Sequence identity value (%; nucleotide/amino acid) for ^a :			
	Pteropodid bats	Insectivorous bats	Other mammals	Human
<i>IFN-α</i> (complete)	91/85	ND	64–81/46–70	78/64
<i>IFN-β</i> (complete)	91–92/83–84	75–81/56–58	66–82/49–72	76/64
<i>IFN-γ</i> (complete)	96/91	81/69	59–83/41–75	76/61
<i>ISG54</i> (partial)	93/88	77–80/68–72	70–81/56–70	82/71
<i>ISG56</i> (partial)	77–94/69–93	80/73	67–84/57–78	79/71
<i>IFN-λ</i> (complete)	91/88	ND	74–80/63–74	79/68
<i>MAVS</i> (partial)	91/88	75–77/63–65	62–78/48–66	69/54
<i>TOMM70</i> (partial)	99/100	96/99	92–96/95–99	96/99
<i>TMEM173</i> (partial)	94/92	85–89/80–86	71–87/77–82	83/76

^aND, not determined.

Given the apparent resistance of bats to illnesses caused by filoviruses and a spectrum of other pathogens (33–35) and a connection between the virulence of filoviruses and suppression of innate immune responses in primates, we investigated EBOV and MARV infections in bat and human cells with a specific focus on IFN responses. We used cell lines from Egyptian rousette bats, as this species was shown to be susceptible to MARV but refractory to EBOV infections *in vivo* (29–32, 36). Because of the critical role of VP35 and VP24 IID in the suppression of innate immune functions, we further employed viruses with IIDs disabled by point mutations. Our data demonstrated that rousette and human cell lines are equally susceptible to EBOV and MARV, and that the filoviral VP35 IID plays a major role in antagonism of the IFN response in bat cells. However, important differences were identified in the innate immune responses of bat cells compared to human cells, as well as asymmetric effects of filoviral IIDs, suggesting that efficient innate antiviral defense contributes to the lack of filovirus pathogenicity in bats.

RESULTS

Innate immune genes of Egyptian rousette cells demonstrated only a limited sequence similarity to human counterparts. To generate expression vectors for rousette IFNs and to develop quantitative reverse transcription-PCR (qRT-PCR) assays for genes involved in the innate immune responses, we first determined the sequences of rousette IFNs and several other innate immune genes. Degenerate primers were designed to amplify these genes based on mammalian counterpart gene sequences available in GenBank. RT-PCR was employed to amplify, clone, and verify the selected genes from rousette cellular RNA. The comparison of the identified sequences with those of other mammals demonstrated that genes of the Egyptian rousette are most similar to the genes of two pteropodid bats, *Pteropus alecto* and *P. vampirus* (Table 1, Fig. 1; see also Fig. S1 in the supplemental material). They next clustered with genes of insectivorous bats (*Eptesicus fuscus*, *Myotis* species, *Rhinolophus* species). In most of the phylogenetic reconstructions, the bat cluster was well separated from the clusters formed by genes of other mammals. A notable exception was the phylogeny of the mitochondrial import receptor subunit TOMM70A, which demonstrated high sequence identity values across different groups of mammals, and the analysis tree did not place bat TOMM70A into a monophyletic cluster (Fig. S1H). The relatively low sequence identity values between rousette innate immune genes and those from nonchiropteran mammals (Table 1) was the likely explanation for the lack of antigenic cross-reactivity of bat proteins with the available antibodies to human proteins (I. V. Kuzmin and A. Bukreyev, data not shown). Furthermore, the sequence distinctions suggest that the mechanisms by which filoviruses antagonize the innate immune response in bats and humans is not identical.

Bat type I IFNs induce an innate immune response in both bat and human cells, whereas bat type II IFN only stimulates a response in rousette cells. Our next question was whether bat IFNs would induce innate immune responses in bat and

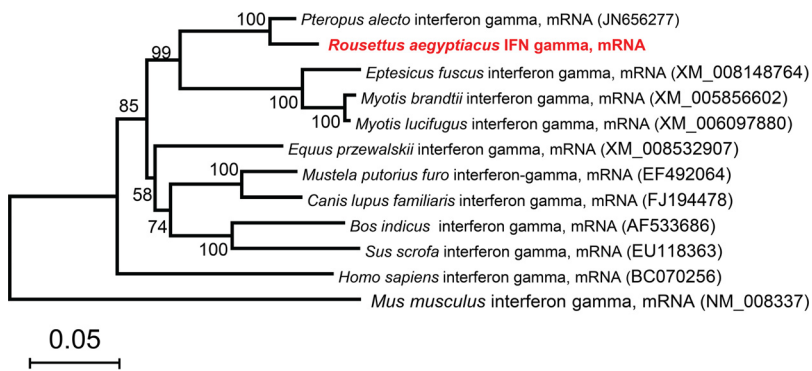


FIG 1 Innate immune genes of Egyptian rousette bats demonstrate only a limited sequence identity to human counterparts. A phylogenetic neighbor-joining tree of *IFN-γ* mRNA is shown. Bootstrap values (1,000 replicates) are present at the nodes, and sequence generated during this study is shown in red.

human cells. We constructed plasmids expressing rousette *IFN-α*, *IFN-β*, and *IFN-γ* and transfected these into rousette cell lines R06EJ and RoNi7. To evaluate biological effects of bat IFNs in a heterologous host species, which is important in the broad context of this study, we also transfected these plasmids into the human cell lines HepG2 and 293T. Both rousette cell lines transfected with *IFN-α*, *IFN-β*, or *IFN-γ* demonstrated increased expression of ISG54 (2.8- to 36.8-fold; $P < 0.05$) and ISG56 (6.4- to 64.8-fold; $P < 0.01$) compared to cells transfected with the empty vector. Interestingly, we frequently observed negative effects of overexpression of one IFN on the expression of other endogenous IFNs. For example, cells transfected with *IFN-α* decreased the expression of *IFN-γ*, whereas cells transfected with *IFN-γ* decreased the expression of *IFN-α* and *IFN-β* (Fig. 2A and B). This phenomenon of interference between different IFNs was previously described (37, 38) and was not unexpected.

We next compared the innate immune response to overexpression of bat IFNs in human cells. The qRT-PCR C_T values for the transfected bat genes, as well as the differences between RNA and DNA signals (no-RT control), were similar in bat and human cells. Human cells demonstrated increased expression of IFN-stimulated genes in response to transfection with bat *IFN-α* and *IFN-β* (Fig. 2C and D). Generally, the two human cell lines responded to the transfection of bat *IFN-α* and *IFN-β* similarly to bat cells, as we detected the increased expression of ISG54 (10.1- to 44.8-fold; $P < 0.05$), ISG56 (74.21- to 98.9-fold; $P < 0.01$), and STAT1 (8.1- to 11.3-fold; $P < 0.05$). In addition, HepG2 cells increased expression of *IFN-λ* (9.9- to 12.2-fold; $P < 0.05$), which was not observed in 293T cells. However, transfection of human cells with bat *IFN-γ* resulted in a very limited induction of innate immune genes (0- to 2.6-fold).

For comparative purposes we transfected human cells with human IFNs, which resulted in a stronger response than was detected for bat IFNs (Fig. 2E and F). For example, HepG2 and 293T cells transfected with human *IFN-α* or *IFN-β* increased expression of ISG54 (42- to 160-fold; $P < 0.01$) and ISG56 (136- to 510-fold; $P < 0.001$), which was 4 to 50 times greater than the response to bat IFNs. The increase of STAT1 and *IFN-λ* expression was approximately the same as that in the cells transfected with bat IFNs (8.2- to 11.8-fold and 10.1- to 13.4-fold, respectively; $P < 0.05$). On the other hand, the response of both HepG2 and 293T cells to human *IFN-γ* was much more limited. These data suggest that the effects of *IFN-γ* are more host species specific than the effects of type I IFNs.

Susceptibility of bats to filoviruses is not determined at the cellular level.

Recent *in vivo* experiments demonstrated that Egyptian rousette bats are susceptible to MARV (30–32) but refractory to EBOV (29, 36). Therefore, we were interested in assessing the susceptibility of two rousette cell lines, R06EJ and RoNi7, to EBOV and MARV in comparison with two human cell lines, HepG2 and 293T. Following infection with recombinant wild-type EBOV encoding enhanced green fluorescent protein (eGFP) (wt EBOV) (39) at a multiplicity of infection (MOI) of 2 PFU/cell, rousette cells demon-

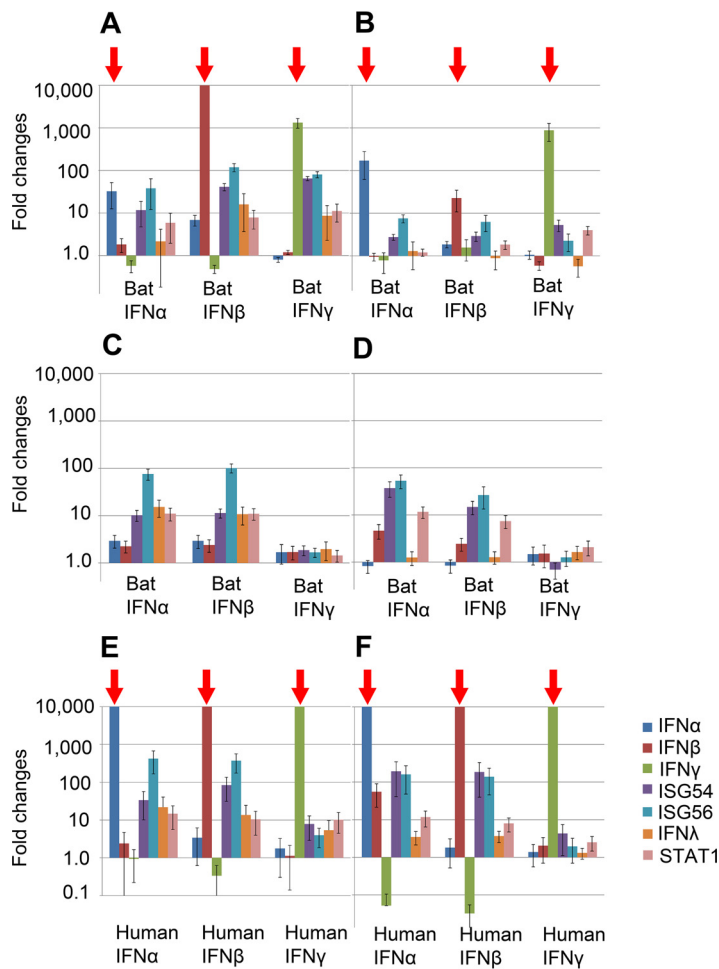


FIG 2 Bat type I IFNs induce innate immune responses in both bat and human cells, while bat type II IFN induces responses only in bat cells. Uninfected cells were transfected with plasmids expressing IFNs as indicated under each plot. Shown are fold changes of selected transcripts 24 h posttransfection compared to cells transfected with the empty plasmid vector. Red arrows indicate the transfected genes whose concentration reflects both RNA resulting from gene expression and the residual plasmid DNA that could not be removed efficiently by DNase I treatment. Mean values with SD based on triplicate samples are shown. (A) RO6EJ cells; (B) RoNi/7 cells; (C and E) HepG2 cells; (D and F) 293T cells.

strated virus replication, as evidenced by eGFP⁺ cells at 24 h postinfection (Fig. 3). The RO6EJ cells demonstrated a moderate susceptibility, with ~10% eGFP⁺ cells. In contrast, susceptibility of RoNi/7 cells was low, with eGFP signal observed in only a small proportion of infected cells (Fig. 3). Susceptibility of HepG2 cells was very high, with >50% eGFP⁺ cells at 24 h postinfection, whereas that of 293T was somewhat lower, with 2 to 5% eGFP⁺ cells (Fig. 4A). Analysis of viral genomic RNA in the infected cells by qRT-PCR and plaque titration of culture media collected at 48 h postinfection confirmed viral replication in bat cell lines. Consistent with the results of fluorescence microscopy, the highest viral titers were documented in HepG2 cells, followed by RO6EJ and RoNi7. Susceptibility of the cells to a biological isolate of MARV from a human in Uganda [MARV-Uga(h)] was only assessed by qRT-PCR and virus titration, because this virus does not encode eGFP (Fig. 5). Both assays demonstrated virus replication in all cell lines.

To confirm that susceptibility of roussette cells to EBOV was not associated with the high infectious dose used for inoculation, we performed an additional experiment inoculating roussette and human cells with several additional strains of EBOV and MARV at an MOI of 0.1 PFU/cell. The results (Fig. 6) corroborated our initial observation that

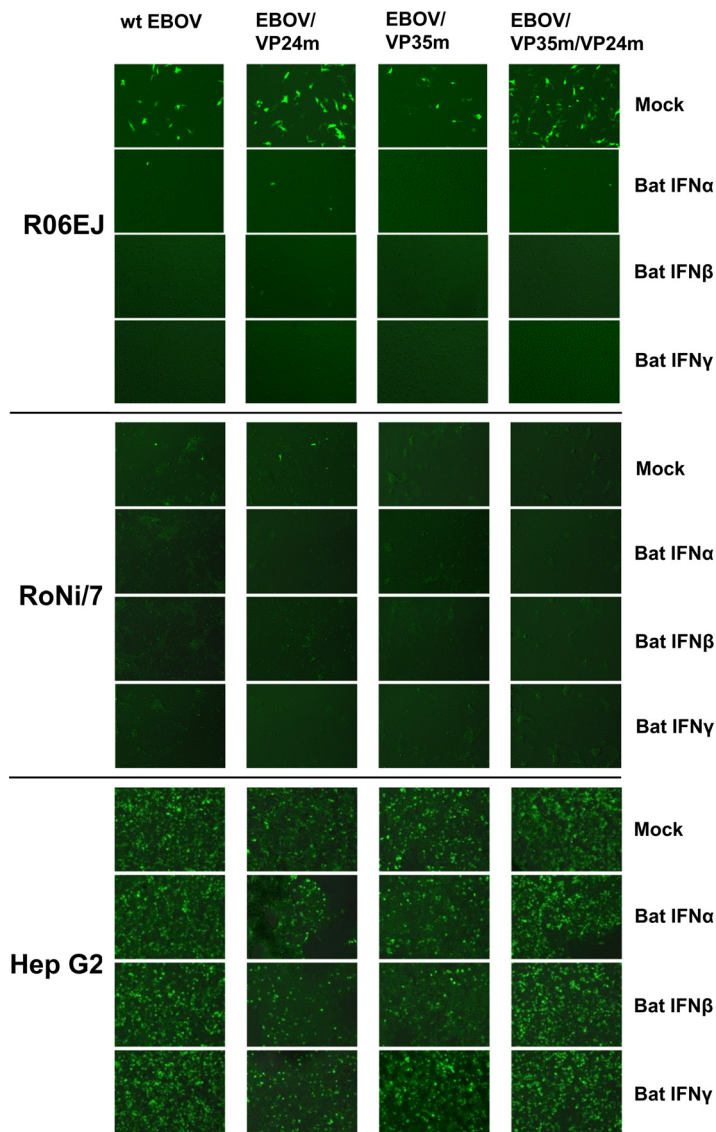


FIG 3 Susceptibility of Egyptian rousette and human cells to wt and mutated EBOV and effects of overexpressed bat IFNs. Cell monolayers in six-well plates were transfected with either empty vector (mock) or plasmids expressing IFN- α , IFN- β , or IFN- γ of Egyptian rousette bats, and 24 h later they were infected with the indicated viruses at an MOI of 2 PFU/cell. After a 1-h-long adsorption at 37°C, cells were washed 3 times with PBS and fresh medium was added to the wells. The photographs were taken 24 h postinfection using a fluorescence microscope with a 20 \times objective.

cells of Egyptian rousette bats are equally susceptible to EBOV and MARV and do not differ in this regard from human cells.

Thus, despite the resistance of Egyptian rousette bats to EBOV, their cells support replication of this virus at levels similar to those of MARV, for which these bats serve as the natural hosts. Moreover, both filoviruses replicate in bat and human cells at comparable levels. Therefore, susceptibility of bat cells to EBOV, and perhaps to filoviruses in general, does not predict host specificity at the organism level.

Filoviruses induce a robust innate immune response in rousette cells, whereas the response of human cells is variable. As the next step, we compared the innate immune responses of bat and human cells to EBOV and MARV infections. Cells were infected with wt EBOV and MARV-Uga(h) at an MOI of 2 PFU/cell, and expression of selected genes involved in the innate immune response was assessed by qRT-PCR at 24 and 48 h. At 24 h postinfection with wt EBOV, the levels of expression of IFNs and

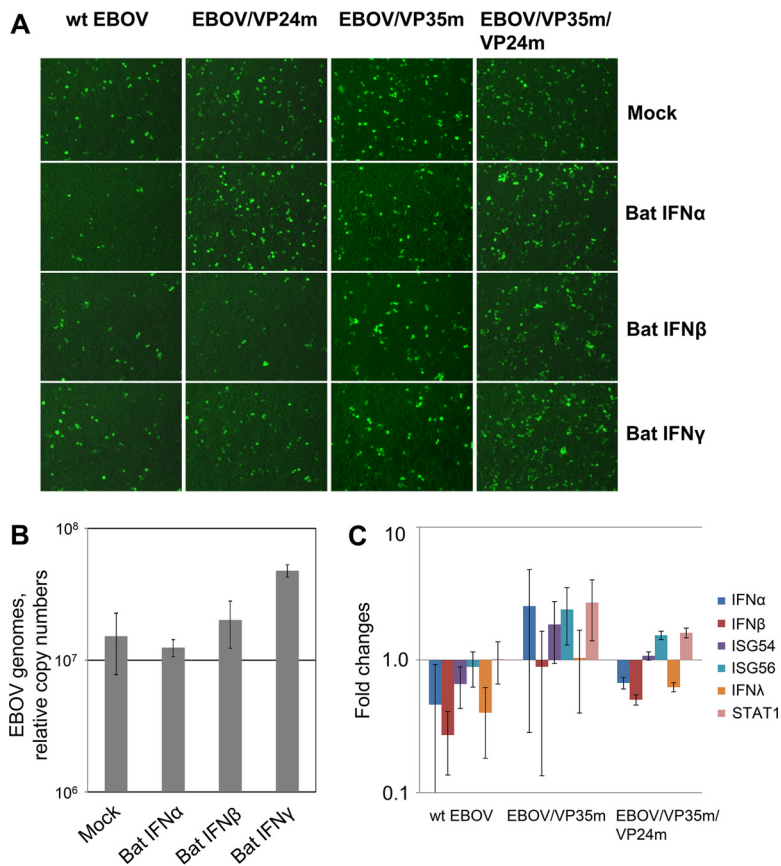


FIG 4 Susceptibility of human 293T cells to wt and mutated EBOV, effects of overexpressed bat IFNs, and induction of innate immune response genes. The experiment was performed as described in the legend to Fig. 3. (A) Cell monolayers at 24 h postinfection. The images were taken using a fluorescence microscope with a 20 \times objective. (B) Relative copy numbers of wt EBOV genome determined by qRT-PCR. Mean values \pm SD based on triplicate samples are shown. (C) Expression of innate immune response genes after infection with wt EBOV and EBOV mutants.

IFN-stimulated genes did not change substantially in R06EJ cells and decreased in RoNi/7 cells. In contrast, MARV-Uga(h) induced an innate immune response in rousette cells (Fig. 7A and C). For example, expression of IFN- γ and IFN- λ was detected in R06EJ cells after infection with MARV-Uga(h) but not with wt EBOV. Moreover, the expression of ISG54 and ISG56 was greater in MARV-infected R06EJ cells than in EBOV-infected cells by 3.1- \pm 0.55-fold ($P < 0.05$) and 3.8- \pm 0.83-fold ($P < 0.05$), respectively, and in infected RoNi/7 cells by 12- \pm 6.9-fold ($P < 0.05$) and 140- \pm 42.8-fold ($P < 0.001$), respectively. Forty-eight hours postinfection, expression of IFN- β , ISG54, and ISG56 increased between 6- and 14-fold in R06EJ cells infected with either wt EBOV or MARV-Uga(h) (Fig. 7B) and less profoundly, but still significantly ($P < 0.05$), in RoNi/7 cells (Fig. 7D). Both rousette cell lines infected with either EBOV or MARV demonstrated 3.5- to 24.6-fold increases of IFN- λ expression ($P < 0.05$). IFN- γ was still increased in R06EJ cells infected with MARV but not with EBOV (Fig. 7B).

In contrast, human HepG2 and 293T cells demonstrated inconsistent innate immune responses to wt EBOV and MARV-Uga(h). At 24 h postinfection, we observed an approximately 2-fold decrease, rather than increase, of IFN- α and IFN- β expression compared to control constitutive levels, whereas at 48 h, there was only a 1.4- to 2.2-fold increase compared to the control (statistically insignificant) (Fig. 4C and 7E and F). Moreover, no significant changes in the expression of ISG54, ISG56, and IFN- λ were observed in these human cells infected with the wild-type viruses at either time point.

In order to confirm whether the same patterns of innate immune response will be applicable for additional strains of EBOV and MARV, we infected the same rousette cell

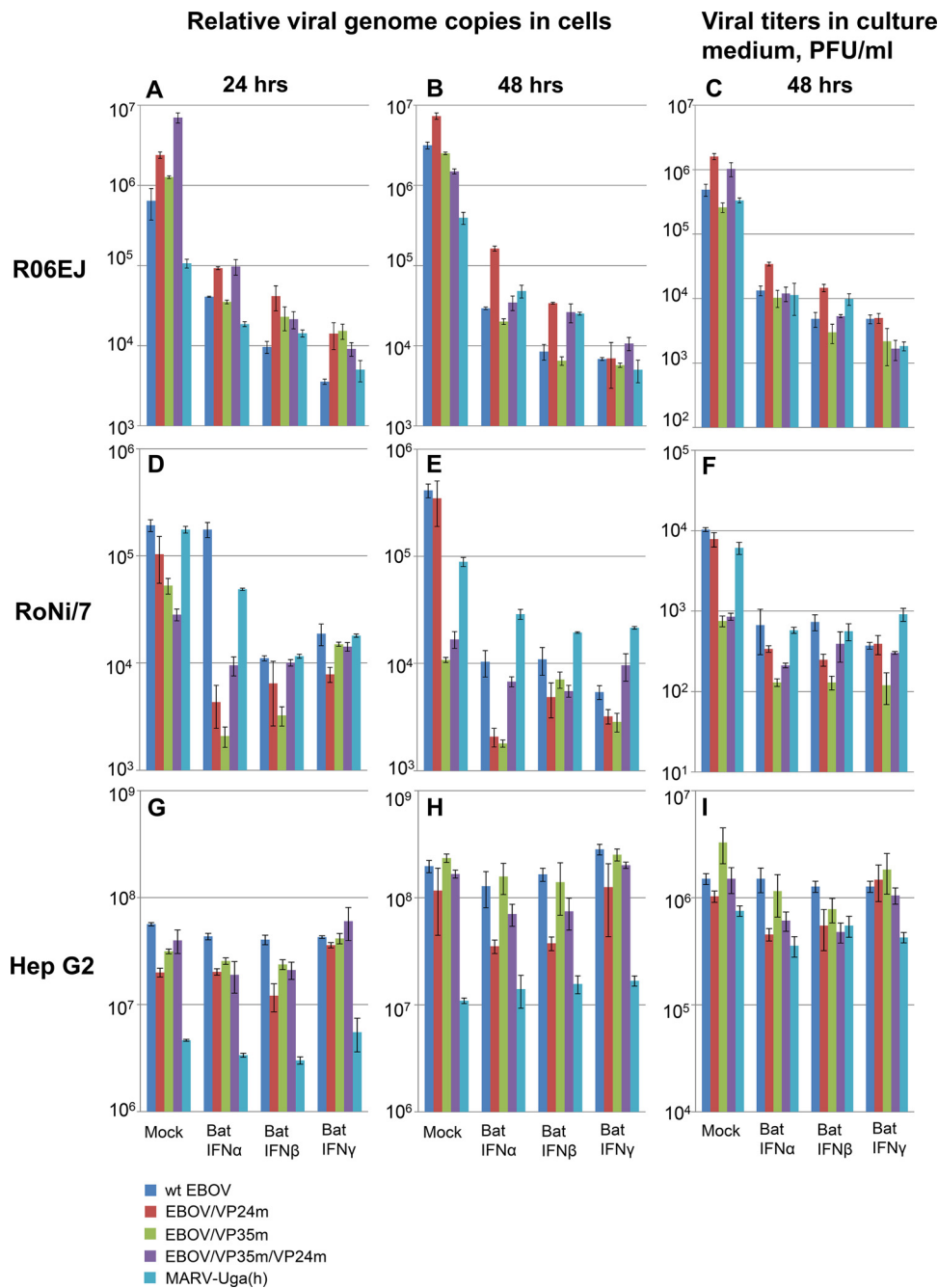


FIG 5 Virus loads in the infected rousette and human cells at 24 and 48 h postinfection at an MOI of 2 PFU/ml. The experiment was performed as described in the legend to Fig. 3. Mean values \pm SD based on triplicate samples are shown.

lines and human cell lines HepG2 and 769p with biological isolates of EBOV, strain Kikwit (EBOV-Kik), and Makona (EBOV-Mak), along with bat-derived recombinant MARV from Uganda [MARV-Uga(b)] and a biological isolate strain Angola (MARV-Ang) at an MOI of 2 PFU/cell (see details on the origin and passage history of each virus in Materials and Methods). We also used a recombinant Newcastle disease virus (NDV) as a reference for which we expected a strong innate immune response (40). The 769p cell line, originating from human kidney cells, was used in place of 293T cells since it demonstrated a stronger immune response. This cell line therefore represents another relevant comparison for rousette kidney cell line RoNi/7. We harvested cells 24 and 48

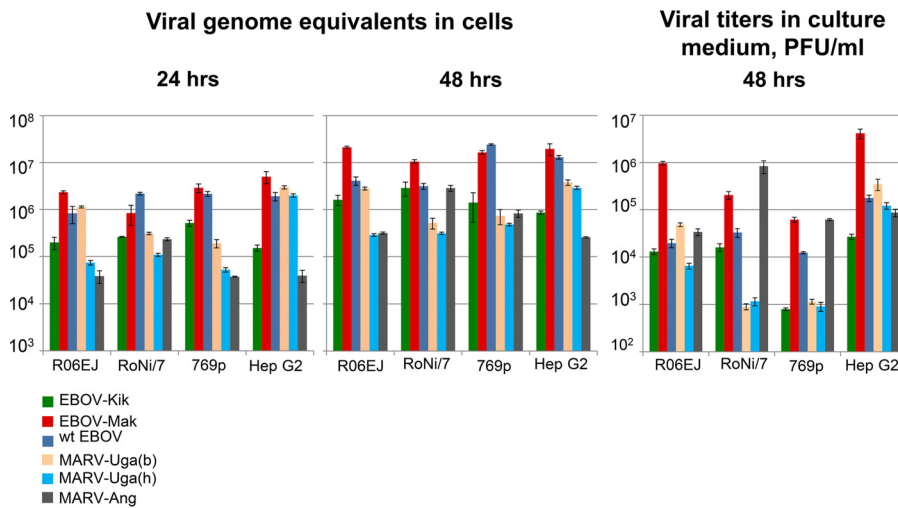


FIG 6 Virus loads in the infected rousette and human cells at 24 and 48 h postinfection at an MOI of 0.1 PFU/cell. The experiment was performed as described in the legend to Fig. 3, except that the MOI was different. Mean values \pm SD based on triplicate samples are shown.

h postinfection and determined expression levels of ISG56 as one of the strong indicators of type I interferon response.

The results (Fig. 8) demonstrated the same expression patterns of ISG56 in response to both EBOV strains in bat cells and in human HepG2 cells. Surprisingly, 769p cells demonstrated upregulation of ISG56 in response to infection with EBOV-Kik to levels similar to those detected in bat cells. EBOV-Mak did not cause such effect and continued to suppress innate responses in both human cell lines but not in bat cell lines. Even more surprising was the observed variability of responses to infection with different strains of MARV. Infection with MARV-Uga(b) resulted in strong upregulation of ISG56 in both rousette cell lines and in human 769p cells as early as 24 h postinfection. The levels of ISG56 in response to infection with this virus were comparable to those observed for NDV infection. In contrast, MARV-Ang caused ISG56 expression patterns similar to those observed for infection with EBOV, although 48 h postinoculation both rousette cell lines and human 769p (but not HepG2) cells demonstrated a strong response.

Taken together, these data demonstrate that both bat cell lines develop a strong innate immune response to filovirus infections whereas the response of human cells to filoviruses is highly variable, ranging from a complete lack of induction of innate immune gene transcription in HepG2 and 293T cells to a robust response in 769p cells. The data also demonstrate that, in contrast to EBOV, which caused similar patterns of innate responses in all cell lines regardless of the strain used, different strains of MARV demonstrated a wide variability in response.

EBOV suppresses innate immune responses in rousette cells more effectively than MARV. To further investigate the differences in response of rousette cells to filoviruses, we profiled by deep sequencing the transcriptomes of R06EJ and RoNi/7 cells at 12 and 24 h postinfection with wt EBOV and MARV-Uga(h). Mapping of sequence reads resulted in identification of 11,488 and 11,523 unique genes in R06EJ and RoNi/7 cells, respectively. These included 642 genes annotated as being involved in the innate immune response in humans. However, only 6.8% of such genes expressed in R06EJ cells and 13.3% of those expressed in RoNi/7 cells demonstrated up- or downregulation in response to filovirus infection compared to uninfected cells (Fig. 9). Downregulation, up to 40 to 60%, was observed in a limited proportion of proteasome (PSM) components; regulators of type I and type II IFN responses, i.e., SLC25A6, HLA-C, RPL13A, and CTNNB1; and several other genes involved in different pathways of immune response, such as PSMC3, OTUB1, DDOST, and CFL1. This downregulation

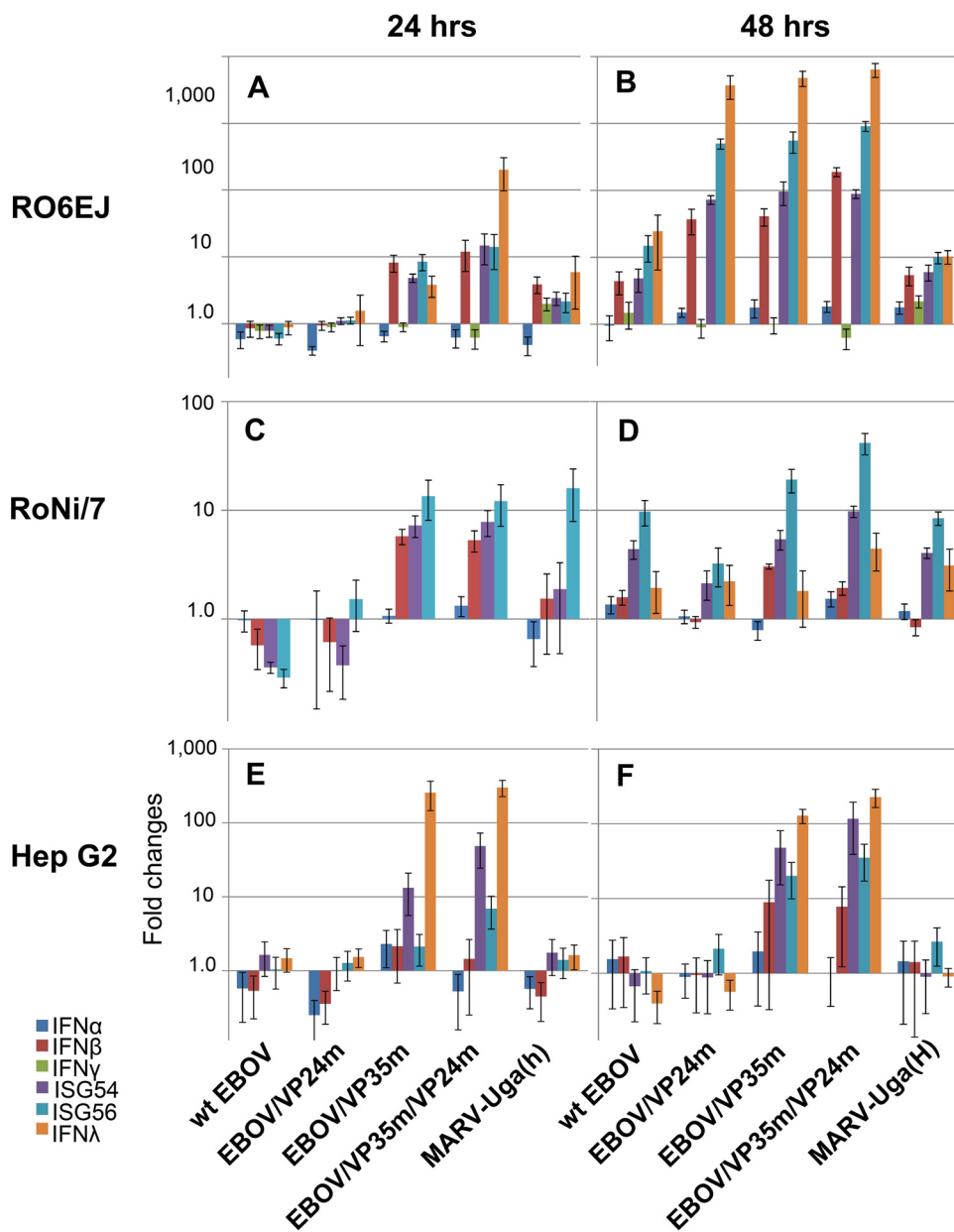


FIG 7 Induction of innate immune response to wt EBOV, MARV-Uga(h), and EBOV mutants with disabled IID in roussette and human cells. See the legends to Fig. 2 and 3 for explanations of the experimental procedure; cells were transfected with an empty plasmid vector rather than plasmids expressing IFNs. The vertical axis shows fold changes of gene expression compared to the level for noninfected cells. Mean values \pm SD based on triplicate samples are shown.

might be a part of the complex response of bat cells to viral infections; however, as shown below, it was more likely associated with functions of filovirus IIDs.

The transcriptome data indicated that infection with wt EBOV triggered little to no innate immune response in roussette cells at the selected time points. In contrast, infection with MARV-Uga(h) triggered a cluster of important innate immune genes, such as MX1, IFIH1, IFITM3, DDX58 (encoding RIG-I), IFIT1 (ISG56), and IFIT2 (ISG54). Most of these genes demonstrated a moderate increase of expression (2- to 4-fold), but IFIT1 was the clear leader, as its expression increased 10.9-fold in R06EJ cells and up to 20.8-fold in RoNi/7 cells infected with MARV-Uga(h) (Fig. 9, Tables S1 and S2). Expression of IFN- α , IFN- β , IFN- γ , and IFN- λ was minimal and demonstrated no significant changes, although induction of IFN- γ was detected at 24 h postinfection with MARV-

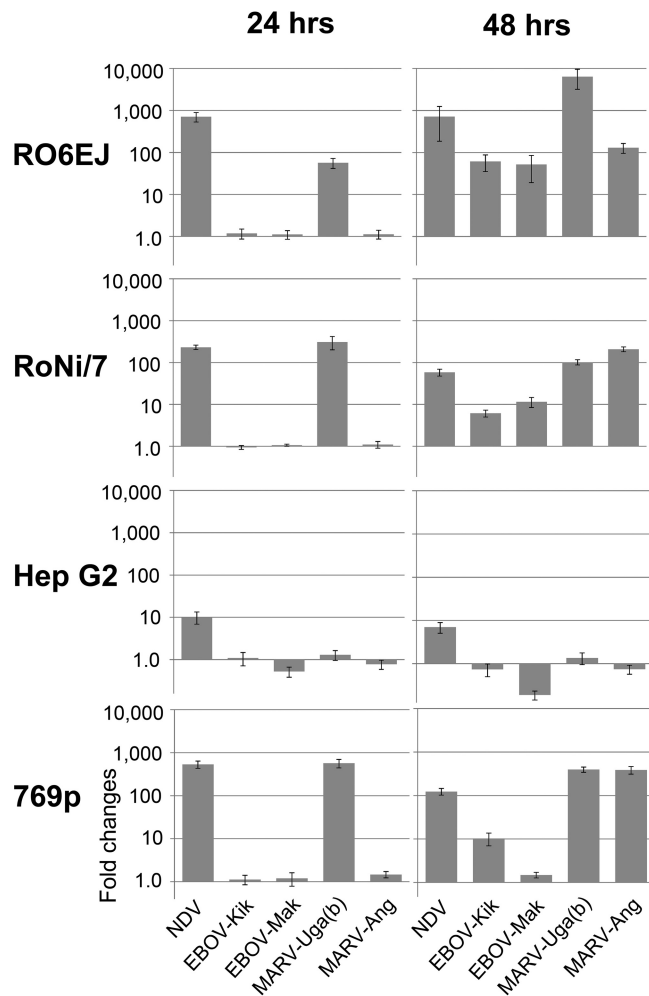


FIG 8 Expression of ISG56 in roussette and human cells infected with NDV, two strains of EBOV, and two strains of MARV. See the legend to Fig. 3 for an explanation of the experimental procedure. The vertical axis shows fold changes of gene expression compared to the level for mock-infected cells. Mean values \pm SD based on triplicate samples are shown.

Uga(h) in R06EJ cells (Fig. 7A, Table 2). The detected upregulation of IFN-stimulated genes implies that IFNs are induced at earlier time points not covered by our sampling. The much lower level of induction of the innate immune response in bat cells by EBOV than by MARV-Uga(h), which has the same infectivity for the cells (Fig. 5 and 6), suggests that generally EBOV suppresses the innate immune response in roussette cells more efficiently than MARV.

Disabling of interferon-inhibiting domains in EBOV proteins similarly unblocks the innate immune response in roussette and human cells. We next determined whether the EBOV IIDs exhibit innate immune antagonistic functions in roussette cells that are similar to those in human cells. Bat and human cells were infected with wt EBOV, EBOV mutants containing point mutations that disable the IIDs, including EBOV/VP24m (substitution K142A in the VP24 protein) and EBOV/VP35m (substitution R312A in the VP35 protein), and the mutant EBOV/VP35m/VP24m, harboring both of these substitutions (15). At 24 h postinfection, we detected a significant induction of innate immune transcripts in R06EJ cells infected with the latter two mutants but not with EBOV/VP24m (Fig. 7A). Specifically, we detected a substantial induction of IFN- β (10.1- to 14.7-fold; $P < 0.05$), ISG54 (6.4- to 19.4-fold; $P < 0.05$), ISG56 (14.5- to 24.2-fold; $P < 0.01$), and IFN- λ (4.39- to 231.8-fold; $P < 0.01$) transcripts. At 48 h postinfection, expression levels of these genes continued to increase; interestingly, at this point,

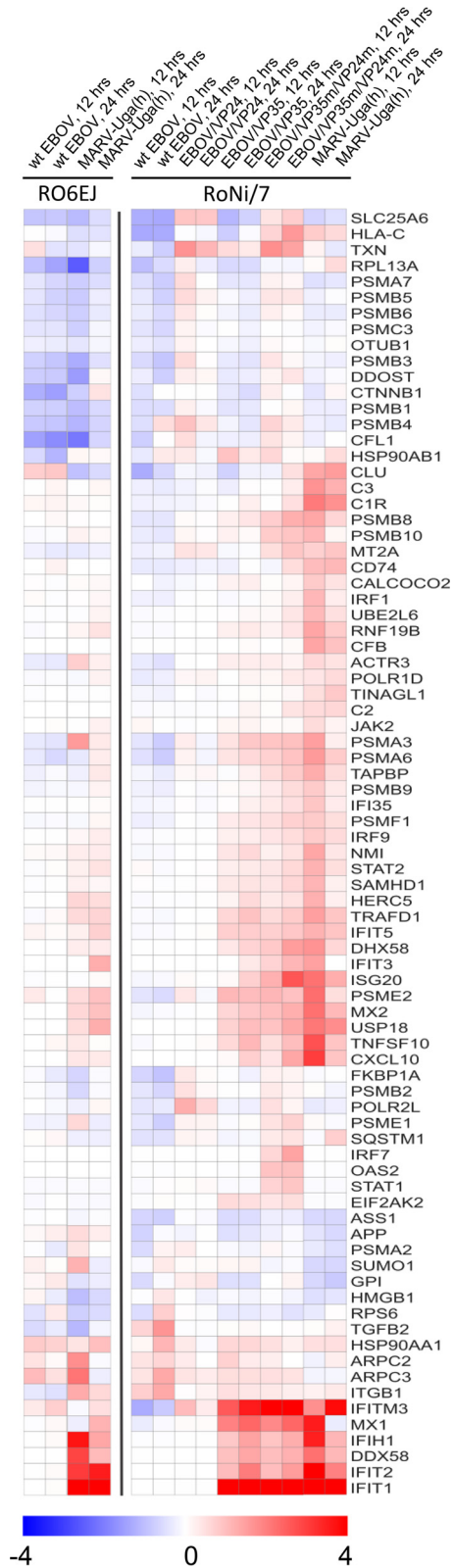


FIG 9 Transcriptome analysis of RO6EJ and RoNi/7 cells infected with wild-type EBOV, MARV, or EBOV mutants with disabled IID. See the legend for Fig. 2 for an explanation of the experimental procedure. The map includes genes involved in innate immune responses which demonstrated differential expression compared to uninfected cells (mean values from two independent samples are shown). The scale bar shows fold changes of gene expression.

TABLE 2 Expression of IFNGR and IFN- γ in bat and human cell lines^a

Cell line and mRNA ^b	Expression level (crude/normalized no. of reads) for ^c :		
	Uninfected	wt EBOV	MARV
HepG2			
IFNGR1	135.6/0.411	162.5/0.369	315.0/0.711
IFNGR2	114.3/0.346	176.5/0.392	351.0/0.778
293T			
IFNGR1	119.5/0.288	115.0/0.386	ND
IFNGR2	145.0/0.336	93.2/0.312	ND
RoNi/7			
IFNGR*	40.0/0.266	0/NA	0/NA
RO6EJ			
IFNGR*	72.0/0.257	0/NA	0/NA
IFN- γ **	45.0/0.183	6.5/0.05	37.0/0.301

^aExpression was determined by transcriptome analysis. Data are (crude/normalized number of reads); mean values from 2 biological replicates are shown.

^b*, IFNGR type not specified; **, other cell lines tested did not express detectable amounts of IFN- γ mRNA.

^cND, not determined; NA, not applicable.

EBOV/VP24m also induced a greater response than wt EBOV (Fig. 7B). In contrast, little to no increase in IFN- α and IFN- γ expression was detected at either time point.

RoNi/7 cells also exhibited a similar induction of innate immune transcripts after infection with EBOV/VP35m and EBOV/VP35m/VP24m but not with EBOV/VP24m (Fig. 7C and D). At 24 h, we detected the increased expression of IFN- β (9.5- to 10.4-fold; $P < 0.05$), ISG54 (46.4- to 50.1-fold; $P < 0.01$), and ISG56 (107.0- to 118.8-fold; $P < 0.01$). At 48 h, expression levels of these genes in the cells infected with either virus were similar, and only marginal levels of IFN- α were detected at both time points. IFN- γ was not expressed in RoNi/7 cells either constitutively or upon infection.

HepG2 cells infected with EBOV/VP35m and EBOV/VP35m/VP24m also demonstrated an induction of the innate response (Fig. 7E and F). At 24 h, infection with these mutants resulted in increased expression of IFN- β (2.8- to 15.6-fold), ISG54 (8.3- to 30.1-fold), ISG56 (2.1- to 6.8-fold) (statistically significant for EBOV/VP35m/VP24m; $P < 0.05$), and IFN- λ (190- to 223.5-fold; $P < 0.001$) compared to infection with wt EBOV. At 48 h, the difference between cells infected with the mutants versus wt EBOV was further increased. HepG2 cells infected with EBOV/VP24m demonstrated the same expression patterns as cells infected with wt EBOV and MARV-Uga(h). The other human cell line tested, 293T, demonstrated a lower induction of the innate immune response to the EBOV mutants compared to wt EBOV, which was mostly associated with EBOV/VP35m (Fig. 4C).

Additional data on unblocking the innate response in rousette cells by disabling EBOV IIDs was obtained via transcriptome analysis of RoNi/7 cells infected with the EBOV mutants (Fig. 9). In agreement with the data obtained by qRT-PCR, disabling of VP24 IID did not rescue the innate immune response. In contrast, disabling of VP35 IID in EBOV/VP35m and EBOV/VP35m/VP24m significantly enhanced the response, which became similar to that observed in the cells infected with MARV-Uga(h). However, several genes downregulated by wt EBOV (the upper part of the heat map) appeared to be induced by both mutants with disabled VP24 IID (EBOV/VP24m and EBOV/VP35m/VP24m) but not EBOV/VP35m or MARV-Uga(h). Therefore, their downregulation, albeit limited, was likely caused by the VP24 IID functions. Taken together, these data suggest that EBOV VP35 and VP24 proteins effectively antagonize the type I IFN response in rousette and human cells.

The VP35 IID but not VP24 IID promotes EBOV replication in rousette cells. To determine if filovirus IIDs promote viral replication in bat cells, we compared viral titers in cells infected with the mutated EBOV versus the cells infected with wt EBOV. In RoNi/7 cells, which were the least permissive to EBOV among our cell lines, we

observed a significantly reduced replication of EBOV/VP35m (6.6- and 60-fold at 24 and 48 h, respectively; $P < 0.001$ based on genome equivalents) and EBOV/VP35m/VP24m (7.2- and 48-fold at 24 and 48 h, respectively; $P < 0.001$) compared to wt EBOV (Fig. 5D to F). Moreover, we did not observe any eGFP⁺ RoNi/7 cells infected with EBOV/VP35m and EBOV/VP35m/VP24m either 24 or 48 h postinfection (Fig. 3), although replication of these viruses still occurred, as evidenced by qRT-PCR analysis of viral genomic RNA in the cells and by titration of culture medium. Unlike the disabling of VP35 IID, disabling of VP24 IID did not show a significant effect on replication of the virus. In R06EJ cells, the difference of RNA loads between different EBOV mutants versus wt EBOV was not substantial; however, EBOV/VP35m titers in supernatants were 1.4 to 1.9 times lower than the titer of wt EBOV ($P < 0.05$). In human cells, the disabling of either IID failed to result in any consistent reduction of virus replication (Fig. 3, 4A, and 5I to K). These data suggest that in bat cells, VP35 IID, but not VP24 IID, effectively promotes EBOV replication, and this effect is greater than that in human cells.

Bat IFNs suppress filovirus replication; the antifilovirus effects of bat and human IFNs are host species specific and do not necessarily depend on ISG54 and ISG56 expression. We next analyzed the effects of bat IFN overexpression on viral replication in bat and human cells. Twenty-four hours after transfection of bat and human cells with bat IFN- α , IFN- β , or IFN- γ , cells were infected with wt EBOV, EBOV mutants, or MARV-Uga(h). The levels of expression of the innate immune genes were analyzed by qRT-PCR at 24 and 48 h. The expression patterns were similar to those in uninfected cells (Fig. 2).

Virus replication, analyzed by qRT-PCR in both bat cell lines transfected with bat IFNs, was significantly reduced (Fig. 3). In culture medium collected from R06EJ cells 48 h postinfection, the reduction of viral titers ranged from 25.2- to 616.8-fold (95% confidence interval [CI], 166.0 ± 72.7 ; $P < 0.01$) compared to the mock-transfected control (Fig. 5C). The relative viral genome copy numbers was decreasing according to the IFN transfected in the order of IFN- γ , IFN- β , and then IFN- α (Fig. 5A and B). Infection of RoNi/7 cells did not show such distinct effects from different IFNs. The reduction of viral titers in these cells ranged from 2.2- to 31.7-fold (95% CI, 12.5 ± 4.7 ; $P < 0.05$) compared to the mock-infected control (Fig. 5D to F). Overexpression of IFNs did not suppress replication of EBOV mutants to a greater extent than replication of wild-type viruses.

Unexpectedly, despite the apparent induction of innate immune transcripts in human cells after transfection of bat type I IFNs (Fig. 2), we did not observe substantial suppression of virus replication. The relative viral genome copy numbers in the HepG2 cells transfected with bat IFN- α or IFN- β decreased by only 1.65- \pm 0.47-fold and 1.67- \pm 0.40-fold, respectively. Similarly, viral titers in culture medium collected 48 h postinfection decreased by only 2.1- \pm 0.6-fold and 2.4- \pm 1.1-fold, respectively. In contrast, transfection of both human cell lines with human type I IFNs decreased virus replication significantly: for IFN- α it ranged from 6- to 15-fold (95% CI, 10.2 ± 3.2 ; $P < 0.05$), and for IFN- β it ranged from 4- to 25-fold (95% CI, 13.6 ± 6.6 ; $P < 0.05$). Human IFN- γ did not reduce viral replication (Fig. 10), which was consistent with the absence of significant induction of the innate immune genes (Fig. 2). Human cells transfected with bat IFN- γ did not show any decrease in virus replication either, as expected (Fig. 3, 4A and B, and 5I to K). We hypothesized that IFN- γ receptors (IFNGR) are present at reduced levels in HepG2 and 293T cells, and this might explain a poor response of these cell lines to overexpression of IFN- γ . We compared IFNGR expression in the transcriptomes of the tested cell lines (Table 2) and found that both HepG2 and 293T expressed IFNGR at levels comparable to those detected in roussette cells. These data suggest that the induction of ISG54, ISG56, and IFN- λ documented in human cells transfected with bat IFNs (Fig. 2) did not efficiently inhibit viral replication. They also demonstrate the host specificity of bat type I IFNs, which induced a strong innate immune response that resulted in a significant reduction of virus replication in bat cells; however, in human cells no reduction of virus replication occurred despite the apparent induction of innate immune genes. In addition, neither bat nor human IFN- γ induced antifilovirus effects in

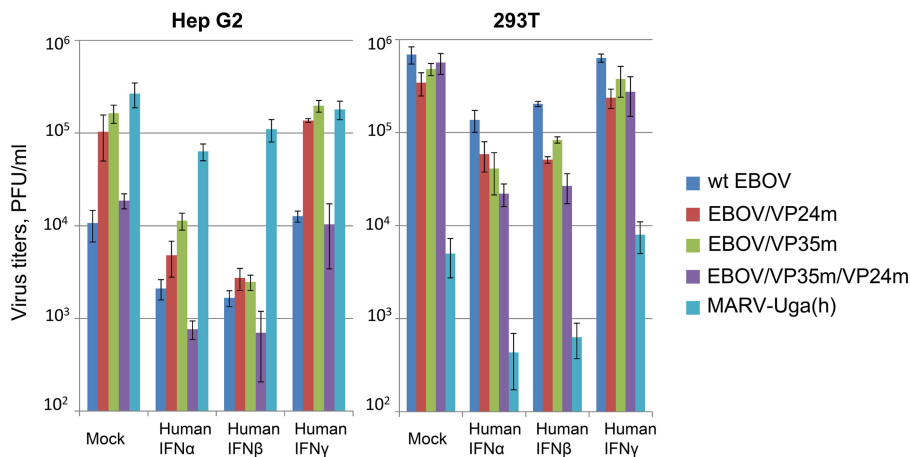


FIG 10 Human type I but not type II IFNs suppress filovirus infection in human cells. Monolayers in six-well plates were transfected with human IFNs or with the empty plasmid vector (mock), and 24 h later they were infected with the indicated viruses at an MOI of 2 PFU/cell. See the legend to Fig. 3 for an explanation of the experimental procedure. Mean values \pm SD based on triplicate samples are shown.

human cells. This was surprising, as in bat cells IFN- γ strongly induced IFN-stimulated genes involved in the type I response and reduced virus replication.

We observed a striking induction of IFN- λ in rousette cells infected with all filoviruses (Fig. 7A, B, and D) and in human cells infected with EBOV mutants (Fig. 7E and F); however, transcriptome analysis revealed only a few reads for IFN- λ receptor genes (IFNLR1) in R06EJ, HepG2, and 293T cells and complete lack of these transcripts in RoNi/7 cells (data not shown). These data suggest that cells of other types also should be used for assessment of IFN- λ effects in bat and human cells.

DISCUSSION

The majority of bat-borne zoonotic viruses that cause severe diseases in humans do not induce significant pathological events in their reservoir hosts, bats (35). The basis for bats’ resistance to virus infections is not understood. While the general characteristics of bat immune systems are similar to those of other mammals (35), some differences have been documented, including a broad distribution of the IFN regulatory factor 7 (IRF7) in bat tissues compared to that in humans, where it is present almost solely within the immune system, or after induction of an IFN- α/β response (41), a broad tissue distribution of the IFN- γ receptors compared to humans (42), the absence or significant reduction of natural killer cell lectin-like receptors (43), the presence of several IFN- ω family members compared to only one in humans (44), and high constitutive expression of IFN- α in various bat tissues (45). Considering that IFN-antagonizing functions of filoviruses have been recognized as major drivers of uncontrolled virus replication and severe clinical disease in humans, it is important to understand how filoviruses interact with the bat innate immune system.

Published experimental studies have demonstrated that Egyptian rousette bats support productive infection, with broad tissue distribution and shedding, with MARV but not EBOV (29, 36). In the current study, we demonstrated that nonimmune cell lines derived from Egyptian rousette bats equally support replication of both MARV and EBOV. Therefore, the resistance of these bats to EBOV does not result from the inability of EBOV to infect their cells. In primates, macrophages and dendritic cells are among the early targets of filoviruses (46). It will therefore be important to determine in future studies how these and other relevant primary bat cells respond to EBOV and MARV infections. Other possibilities, such as different doses and routes of inoculation and specific physiological conditions of bats (reproduction and stress), should also be taken into account to determine whether they can alter the susceptibility of Egyptian rousette bats to EBOV.

Following viral infections, we detected induction of IFN- β in bat cells, whereas the

expression levels of IFN- α did not change (Fig. 7A to D). This observation is in agreement with a recent report (45) that documented an increase of IFN- β but not IFN- α expression in cells of *Pteropus alecto* bats in response to nonspecific stimulations and viral infections. However, in contrast to that report, we observed low constitutive expression levels of IFN- α in roussette cells, both by qRT-PCR and by transcriptome analysis. The threshold cycle (C_T) values of IFN- α and IFN- β obtained in qRT-PCR of uninfected roussette and human cells were similar. Of course, these C_T values cannot be used for direct comparisons given that the reactions were performed with unique primer-probe combinations, which might result in different efficiency of amplification and probe annealing. Furthermore, given the variety of IFN- α classes in bat and human cells, the mRNA of some of these might be recognized in our assays better than others. However, transcriptome sequencing of these cell lines provided very few reads for all subtypes of IFN- α , lower than the total number of reads for IFN- β . It is possible that mechanisms of IFN- α response in bats of different species are quite distinct, consistent with the different organization of the IFN- α locus in bat genomes (47, 48).

The conservation of IID suppressing type I IFN responses, found not only in the EBOV and MARV proteins but also in the proteins of the recently identified filovirus Lloviu (49), suggests that these domains are operative in the natural virus hosts. Consistent with that, our study demonstrated that wt EBOV and MARV suppress the type I IFN responses in Egyptian roussette cell lines, with the exception of MARV-Uga(b), which induced the response as early as 24 h postinfection. The observed different responses of bat cells to different strains of MARV can be related to adaptation of these strains to different bat species, which is documented for other bat-borne viruses, such as rabies (50) and paramyxoviruses (51). However, 48 h postinfection with all wild-type filoviruses, both R06EJ and RoNi/7 cell lines increased expression of IFN-stimulated genes (Fig. 7B and D and 8). In human cells, no response at 24 h was detected, with the exception of MARV-Uga(b) in 769p cells, which was similar to the response of bat cells. At 48 h, HepG2 cells still did not demonstrate substantial innate responses to wild-type filoviruses, but strong induction of ISG56 was detected in 769p cells infected with all viruses except EBOV-Mak.

Disabling of the IID in VP35 or both VP35 and VP24 IID effectively unblocked induction of the innate immune response in bat and human cells as early as 24 h postinfection (Fig. 7). Conversely, disabling of VP24 IID alone unblocked the innate response less prominently and only later during infection. Our observations are consistent with the different effects of EBOV VP24 and VP35 and a later suppressive effect of the former IID documented in human dendritic cells (15, 16), suggesting a stronger suppressive effect of the type I IFN response by VP35 IID compared to that by VP24 IID. More importantly, the data revealed an induction of several interferon-stimulated genes with infection of the EBOV/VP24m and EBOV/VP35m/VP24m viruses but not with wt EBOV, EBOV/VP35m, or MARV (Fig. 9). We observed reduced replication of EBOV/VP35m and EBOV/VP35m/VP24m viruses compared to that of wt EBOV and EBOV/VP24m in the least susceptible RoNi/7 cells (Fig. 3 and 5), which suggested an important role of the VP35 IID for EBOV replication in bat cells. The absence of such effect in the highly susceptible R06EJ (and HepG2) cells might be due to the relatively high virus doses used in our experiments.

Interestingly, we observed suppression of the type II IFN response in R06EJ cells (the only cell line constitutively expressing IFN- γ) infected with all EBOV constructs. In contrast, MARV-Uga(h) stimulated IFN- γ expression in these cells. These data suggest that some presently unknown domains of EBOV, not related to the studied IIDs, are able to inhibit the type II IFN response in bat cells, and that these domains are less powerful in at least some strains of MARV.

A recently published study reported no significant changes in expression of host genes and in induction of pathways relevant for viral infections in R06EJ cells infected with EBOV or MARV (52). However, our study did show induction of multiple genes. For example, we did observe induction of ISG56 by all EBOV strains tested (Fig. 8) and upregulation of genes involved in the DDX58 (RIG-I-like) and JAK/STAT pathways not

only in the cells infected with EBOV mutants with disabled IIDs but also in the cells infected with MARV-Uga(h) (Fig. 9; see also Tables S1 and S2 in the supplemental material). Generally, MARV induced a greater number of innate response genes than EBOV (Fig. 9).

Transfection of roussette cells with each bat IFN not only dramatically increased transcription of IFN-stimulated genes (Fig. 2) but also strongly reduced virus replication (Fig. 5). In contrast, transfection of human cells with bat IFN- α and IFN- β did not significantly decrease virus loads, although it resulted in transcriptional upregulation of several IFN-stimulated genes, suggesting host species-specific antiviral effects of the type I IFNs. Conversely, transfection of human cells with human IFN- α and IFN- β resulted in a stronger upregulation of IFN-stimulated genes and suppressed filovirus replication. Despite the strong induction of ISG54 and ISG56 by bat IFN- α and IFN- β in HepG2 cells, they failed to reduce viral replication. These data led us to conclude that antiviral effects of type I IFNs do not necessarily correlate with the induction of important innate immune genes, such as ISG54 and ISG56, suggesting involvement of some alternative pathways.

Surprisingly, the experiments conducted in human cell lines did not show any substantial response to overexpression of either bat or human IFN- γ (Fig. 2). In agreement with this, no reduction of filovirus replication was observed (Fig. 4A and B, 5E and F, and 10) in human cells transfected with IFN- γ . Transcriptome analysis demonstrated expression of IFN- γ receptors in all tested bat and human cells at approximately the same levels (Table 2), hence the lack of response cannot be explained by the absence of receptors. It is important that overexpression of bat IFN- γ in bat (but not human) cells induced ISG54 and ISG56, which are involved in type I IFN responses. This suggests that the antiviral effect of IFN- γ in bat cells, at least in part, results from interferon cross talk (53, 54) and has a greater biological role than it does in human cells.

Filovirus infection resulted in different patterns of IFN- λ expression in bat and human cells. In uninfected bat cells or bat cells infected with wt EBOV and EBOV/VP24m, IFN- λ was nearly undetectable by qRT-PCR. On the contrary, IFN- λ transcription was increased in the cells infected with EBOV/VP35m, EBOV/VP35m/VP24m, and MARV-Uga(h) (Fig. 7A). IFN- λ expression was dramatically increased in R06EJ cells infected with all viruses (particularly EBOV mutants with disabled IIDs) at 48 h postinfection (Fig. 7B), and a more moderate increase of IFN- λ expression was detected in RoNi/7 cells at this time (Fig. 7D). In human cells, IFN- λ expression was induced earlier but only in response to the EBOV mutants with VP35 IID disabled (Fig. 7E and F). Transfection of bat or human cells with bat IFN- α and IFN- β sharply increased expression of IFN- λ (Fig. 2). We also detected a significant expression of IFN- λ in human cells infected with EBOV mutants (Fig. 7E and F). However, transcriptome analysis demonstrated the absence or very low expression levels of IFN- λ receptors in the tested cell lines. These data suggest that either bat IFN- λ is nonfunctional during filovirus infection or expression of IFN- λ receptors in bats is highly organ specific, and additional cell lines are required to adequately assess its effects. In human cells, IFN- λ R1 expression is limited to hepatocytes, epithelial cells of the lung, intestine, and skin, and cells of myeloid lineage (55–57). A significant but nonfunctional increase of IFN- λ expression, resulting from a disruption of downstream IFN- λ signaling, was reported for human cells infected with influenza virus (11). On the other hand, IFN- λ treatment of bat *Pteropus* cells infected with the orthoreovirus Pulau did reduce viral replication (42).

The study had several limitations. Due to the absence of bat-specific reagents, we could not detect bat proteins in the cells, and we had to rely on the expression levels of their genes. Second, we used immortalized nonimmune cell lines, whereas one of the primary targets of filoviruses are immune cells of monocyte lineages, which may exhibit different patterns of susceptibility, permissiveness, and immune responses. Finally, we focused on a limited number of host genes as markers of the innate immune response and could not assess all parameters of this complex multilateral process. In fact, bats are very diverse, and different species harbor different pathogens, developing distinct

kinds of virus-host interactions, which cannot be easily generalized. Further studies focused on bat immune cells and various nonimmune cells, as well as analysis of tissues from bats of different species infected with filoviruses, will help to overcome these deficiencies.

In conclusion, the study resulted in several important findings. First, cells of Egyptian rousette bats mount robust innate immune responses to filovirus infection. Second, filovirus IIDs are active in both rousette and human cells; however, the VP35 IID plays a greater role in promotion of viral replication in rousette cells than in human cells. Third, IFN- γ plays a greater role in control of filovirus infections in rousette nonimmune cells than in human cells. At least in part, the antiviral effect of IFN- γ results from cross talk leading to activation of the type I IFN response. Fourth, the antiviral effects of rousette and human IFNs do not necessarily correlate with induction of IFN-stimulated genes ISG54 and ISG56. These data are important not only for understanding the interaction of filoviruses with the innate immune system of the reservoir and accidental hosts but also for understanding the factors involved in filovirus evolution in their natural reservoirs.

MATERIALS AND METHODS

Cells and viruses. Two immortalized cell lines, derived from Egyptian rousette bats, were used in the study, including R06EJ (fetus body) (58) and RoNi/7 (adult bat kidney) (59). The R06EJ cells were maintained in Dulbecco's modified Eagle's medium (DMEM)-F-12 GlutaMAX medium, and RoNi/7 cells were maintained in DMEM (Life Technologies, Thermo Fisher Scientific, Waltham, MA) supplemented with 10% fetal bovine serum (HyClone, Thermo Fisher Scientific, Waltham, MA) and antibiotic-antimycotic (Life Technologies, Thermo Fisher Scientific, Waltham, MA) as previously described (58, 59).

The human immortalized cell lines 293T (derived from an embryonal kidney but possibly having an adrenal or neuronal origin reference [60]), HepG2 (hepatocellular carcinoma), and 769p (renal carcinoma) were obtained from the American Type Culture Collection (Manassas, VA). The 293T cells were maintained in DMEM, HepG2 in MEM, and 769p in RPMI 1640 (Life Technologies, Thermo Fisher Scientific, Waltham, MA) supplemented with 10% fetal bovine serum (HyClone) and antibiotic-antimycotic (Life Technologies).

The study utilized recombinant EBOV, strain Mayinga, expressing the enhanced green fluorescent protein (eGFP) gene, referred to as the wild type (wt EBOV); the virus replicates at the same level as its biologically isolated counterpart (39). The study also utilized mutants of this virus with disabled IIDs, EBOV/VP24m (substitution K142A in the VP24 gene), EBOV/VP35m (substitution R312A in the VP35 gene), and the double mutant EBOV/VP35m/VP24m, harboring both of these substitutions. The viruses were recovered as described previously (15, 16) using the full-length clone kindly provided by Jonathan Towner and Stuart Nichol (Centers for Disease Control and Prevention, Atlanta, GA) and passaged three times in Vero E6 cells. EBOV strain 199510621, also known as Kikwit (referred to as EBOV-Kik), was isolated from a human in the Democratic Republic of Congo during the 1995 outbreak (61) and underwent three passages in Vero E6 cells. EBOV strain Makona CO7 (referred to as EBOV-Mak) was provided by Stephan Gunther (Bernhard-Nocht Institute for Tropical Medicine, Hamburg, Germany) through Gary Kobinger (Canadian National Microbiology Laboratory). The virus was recovered from a human in Guinea during 2014 (62) (GenBank accession no. [KJ660347](https://www.ncbi.nlm.nih.gov/nuccore/KJ660347)) and underwent five passages in Vero E6 cells. MARV strain 200702854 Uganda [referred to as MARV-Uga(h)] originally was isolated from a subject designated patient A during the outbreak in Uganda in 2007 (26) and underwent four passages in Vero E6 cells. The recombinant MARV 371Bat2007 [referred to in our study as MARV-Uga(b)] was derived from an isolate obtained from an Egyptian rousette bat captured in Uganda in 2007 (63); the virus was recovered using the reverse genetics system kindly provided by Cesar Albariño and Stuart Nichol (CDC, Atlanta, GA) and underwent three passages in Vero E6 cells. MARV strain 200501379 Angola (referred to as MARV-Ang) was isolated from a human during the outbreak in Angola during 2005 (64) and underwent three passages in Vero E6 cells. The isolates EBOV-Kik, MARV-Uga(h), and MARV-Ang originally were obtained from the Special Pathogens Branch, CDC, and deposited at the World Reference Center of Emerging Viruses and Arboviruses (WRCEVA), housed at UTMB. Recombinant Newcastle disease virus (NDV), encoding eGFP (40), was propagated in LLC MK2 cells in serum-free MEM.

Sequencing of genes involved in the innate immune response in Egyptian rousette bats. To obtain complete or partial mRNA sequences of several selected genes involved in the innate immune response and the glyceraldehyde 3-phosphate dehydrogenase (GAPDH) of the Egyptian rousette bat, we assembled multiple alignments of sequences present in GenBank for other mammalian species, placing available bat sequences on the top of the alignment for foreground consideration. Several pairs of degenerated primers were constructed for RT-PCR amplification of RNA extracted from R06EJ and RoNi/7 cells. The RT-PCR products were purified and sequenced, and the obtained sequences were subjected to BLAST analysis and construction of phylogenetic trees to ensure that they represented the target genes. When the manuscript was in revision, a paper describing the transcriptome of Egyptian rousette bat was published (65) which also helped us verify our sequences.

Construction of plasmids expressing Egyptian rousette IFNs. IFN open reading frames were amplified by nested RT-PCR from R06EJ and RoNi/7 cells, cloned into pCAGGS/MCS plasmid using NotI

and SacI restriction sites, resulting in vectors expressing roussette IFN- α (pCRE-IFNA), IFN- β (pCRE-IFNB), or IFN- γ (pCRE-IFNG), and transformed into DH5 α competent cells (Life Technologies, Thermo Fisher Scientific). Twenty clones encoding IFN- α , 8 clones encoding IFN- β , and 6 clones encoding IFN- γ were sequenced. The IFN- β and IFN- γ sequences were identical in the clones, whereas IFN- α demonstrated a significant variability in both R06EJ and RoNi/7 cells, with all 20 clones harboring at least one substitution. The IFN- α sequence with the greatest similarity to the consensus sequence obtained via direct sequencing of the RT-PCR product was selected for further experiments.

Several polyclonal antibodies to human IFNs did not cross-react with bat IFNs in our Western blotting experiments; therefore, expression of bat IFNs was confirmed by (i) induction of IFN-stimulated genes in cells transfected with IFNs compared to cells transfected with empty pCAGGS/MCS vector and (ii) reduction of filovirus replication in IFN-transfected cells.

Plasmids encoding human IFN- α 1, IFN- β , and IFN- γ were purchased from GenScript (Piscataway, NJ). The IFN sequences from these plasmids were PCR amplified and inserted into the pCAGGS/MCS vector. Expression of human IFNs was confirmed by Western blotting.

Quantitative RT-PCR. We used sequences of bat *IFN- α* , *IFN- β* , *IFN- γ* , *ISG54*, *ISG56*, *IFN- λ* , *MAVS*, and *STAT1* for development and validation of qRT-PCR gene expression assays with GAPDH as a housekeeping gene. Quantitative PCR (qPCR) primers and 6-carboxyfluorescein–minor groove binder (FAM-MGB)-labeled probes were designed using Primer Express 3.0 software (Applied Biosystems, Thermo Fisher Scientific) (sequences can be provided upon request). For RNA extraction, cell monolayers in six-well plates (Costar, Corning) were washed twice with 1.0 ml of 0.1 M phosphate-buffered saline (PBS; Mediatech, Corning, Manassas, VA) and denatured in 0.8 ml of TRIzol reagent (Ambion, Thermo Fisher Scientific). After phase separation with chloroform, the aqueous fraction was mixed with an equal volume of 100% ethanol and subjected to RNA extraction using a Direct-Zol RNA miniprep kit (Zymo Research, Irvine, CA) according to the manufacturers' recommendations, with on-column DNase 1 treatment. The concentration of the extracted RNA was measured with a NanoDrop 2000 (Thermo Fisher Scientific) and adjusted to 80 to 150 ng/ μ l. The reactions were performed in 384-well format with the TaqMan RNA-to-Ct one-step kit (Applied Biosystems, Thermo Fisher Scientific) on the 7900HT real-time PCR thermal cycler (Applied Biosystems, Thermo Fisher Scientific) using the recommended parameters (48°C for 15 min, 95°C for 10 min, and 40 cycles of 95°C for 15 s and 60°C for 1 min).

All samples were run in triplicate. Standard curves were constructed and slopes determined for all genes of interest in at least two independent runs. Contamination with genomic DNA was ruled out with the no-RT control. The relative expression rates, standard deviations (SD), and 95% CI corrected for PCR efficiency were determined with REST-384 software (66; <http://rest.gene-quantification.info>). All bat genes of interest produced suitable C_T values for quantitative interpretation except IFN- γ and IFN- λ . The IFN- γ mRNA was detected in R06EJ cells only. The IFN- λ mRNA was present in naive and mock-transfected R06EJ and RoNi/7 cells close to the lower detection limits (C_T of >30), and therefore the expression changes could not be quantified accurately in many instances, particularly at 24 h postinfection. This was not an issue for human cell lines with high constitutive expression levels of IFN- λ .

For comparative quantitative analysis of viral genome copies, primers and probes for the NP genes of EBOV and MARV were constructed as described above. A known number of molecules of a synthetic DNA oligonucleotide encompassing the PCR-amplified fragment was serially diluted and used for creation of standard curves. This approach did not include *in vitro* reverse transcription and was directly used to determine the numbers of viral cDNA copies. However, as all extraction and reaction procedures were performed using the same techniques, this approach for comparative determination of relative viral genome copy numbers between samples is justified.

When bat IFNs were transfected into cells, the plasmid DNA could not be completely removed during RNA purification, as was evidenced by the residual DNA signal in qRT-PCR (as indicated in Fig. 2). However, differences between C_T values obtained after RT reaction (RNA signal) and the no-RT control (DNA signal) ranged from 9 to 17 cycles. Since every 3.3 cycles corresponded to an \sim 10-fold decrease in copy numbers, over 99.9% of qRT-PCR result resulted from RNA.

Transfections and infection experiments. Cells were seeded in six-well plates at a density that ensured formation of 80 to 90% confluent monolayers in 24 h. At this time the cells were transfected with plasmids expressing bat IFNs or control plasmids using TransIT-LT1 (Mirus Bio LLC, Madison, WI) according to the manufacturer's recommendations. All tests were performed in triplicate. At 24 h posttransfection, cells were infected with wt EBOV, EBOV/VP24m, EBOV/VP35m, EBOV/VP35m/VP24m, or MARV-Uga(h) at a multiplicity of infection (MOI) of 2 PFU/cell (as determined in Vero E6 cells) in a volume of 2.0 ml. After 60 min of adsorption at 37°C the inocula were removed, and cells were washed three times with PBS, supplied with 2.0 ml of fresh medium, and incubated at 37°C in a 5% CO₂ humidified atmosphere. In a series of additional experiments, nontransfected cells were infected with an extended panel of filoviruses and NDV at an MOI of 0.1 or 2 PFU/cell by following the same protocol. Cell monolayers were harvested in TRIzol reagent 24 and 48 h postinfection for analysis of gene expression and viral loads via qRT-PCR, and culture medium was collected 48 h postinfection for virus titration. Titrations were performed by a plaque assay in Vero E6 cells in 96-well format by counting fluorescent plaques under the microscope for eGFP-expressing EBOV constructs or in 24-well format with immunostaining for the viruses that do not express eGFP.

Transcriptome analysis of filovirus-infected roussette cells. R06EJ and RoNi/7 monolayers in 6-well plates were infected as described above and harvested in TRIzol reagent 8, 12, or 24 h postinfection. The extracted total RNA was processed for selection of poly(A)-tailed mRNA using NEBNext oligodeoxythymidine magnetic beads (New England BioLabs, Ipswich, MA), followed by fragmentation and first- and second-strand synthesis using a NEXTflex rapid Illumina directional transcriptome sequencing (RNA-Seq)

library preparation kit (Bioo Scientific Corp., Austin, TX) and purification with Agencourt AMPure XP magnetic beads (Beckman Coulter, Brea, CA). cDNA libraries were created using random hexamers and ligated with NEXTflex RNA-Seq barcodes (Bioo Scientific Corp., Austin, TX). cDNA fragments of 75 to 80 nucleotides were sequenced on the Illumina NextSeq 500.

We started with transcripts assembled by the Trinity package using data from an unrelated project with *Myotis* bat transcriptome. We used this database and our own software to build a nonredundant *Rousettus aegyptiacus* transcript database for this study. The database included all variants as long as they differed by at least 15% of length from any member in the database, always favoring the longer variant in the case of a choice. Each read from the experiment was mapped to this set of bat transcripts using BLAST (GenBank). The mappings were allowed to have gapped matches along with mismatches. The best match was used for each read. Transcripts were assigned a median coverage value based on the distribution of mappings of reads across the length of the transcript. The median coverage across the transcript was used as an estimate of gene expression. The expression values were normalized to the total number of reads mapping to mRNA transcripts in each sample, so that each sample had a total of 10 million reads. The log ratios between the expression values of infected and noninfected samples were calculated to identify genes that were up- or downregulated. The expression values were regularized by adding noise (value, 5) to each gene's expression level before the log ratios were calculated to ensure that genes with low expression did not contribute to the list of genes with large fold changes. An absolute natural log ratio of 0.2 was used as the cutoff. The heat map for \log_2 -transformed normalized values was generated using Morpheus software (<https://software.broadinstitute.org/morpheus>).

BSL-4 work. All work with EBOV and MARV was performed within the Galveston National Laboratory biosafety level 4 (BSL-4) laboratories.

SUPPLEMENTAL MATERIAL

Supplemental material for this article may be found at <https://doi.org/10.1128/JVI.02471-16>.

TEXT S1, PDF file, 0.1 MB.

TEXT S2, PDF file, 1.2 MB.

ACKNOWLEDGMENTS

This study was supported by the Defense Threat Reduction Agency (DTRA), grant HDTRA1-14-1-0013, "Comparative immunology of *Rousettus aegyptiacus* reservoir with filoviruses," to C.B. and A.B.

Rousette cell line RoNi/7 was generated by Marcel A. Müller and Christian Drosten, Institute of Virology, University of Bonn Medical Centre, Bonn, Germany, and provided within the framework of EU-FP7 ANTIGONE (no. 278976) and the German Research Council (DR 772/10-2). Ebola virus strain Makona CO7 was provided by Stephan Gunther (Bernhard-Nocht Institute for Tropical Medicine, Hamburg, Germany).

REFERENCES

- Rougeron V, Feldmann H, Grard G, Becker S, Leroy EM. 2015. Ebola and Marburg haemorrhagic fever. *J Clin Virol* 64:111–119. <https://doi.org/10.1016/j.jcv.2015.01.014>.
- Feldmann H, Geisbert TW. 2011. Ebola haemorrhagic fever. *Lancet* 377: 849–862. [https://doi.org/10.1016/S0140-6736\(10\)60667-8](https://doi.org/10.1016/S0140-6736(10)60667-8).
- Wong G, Kobinger GP, Qiu X. 2014. Characterization of host immune responses in Ebola virus infections. *Expert Rev Clin Immunol* 10:781–790. <https://doi.org/10.1586/1744666X.2014.908705>.
- Messaoudi I, Amarasinghe GK, Basler CF. 2015. Filovirus pathogenesis and immune evasion: insights from Ebola virus and Marburg virus. *Nat Rev Microbiol* 13:663–676. <https://doi.org/10.1038/nrmicro3524>.
- Pestka S, Krause CD, Walter MR. 2004. Interferons, interferon-like cytokines, and their receptors. *Immunol Rev* 202:8–32. <https://doi.org/10.1111/j.0105-2896.2004.00204.x>.
- Platanias LC. 2005. Mechanisms of type-I and type-II-interferon-mediated signalling. *Nat Rev Immunol* 5:375–386. <https://doi.org/10.1038/nri1604>.
- Ben-Asouli Y, Banai Y, Pel-Or Y, Shir A, Kaempfer R. 2002. Human interferon-gamma mRNA autoregulates its translation through a pseudoknot that activates the interferon-inducible protein kinase PKR. *Cell* 108:221–232. [https://doi.org/10.1016/S0092-8674\(02\)00616-5](https://doi.org/10.1016/S0092-8674(02)00616-5).
- Rhein BA, Powers LS, Rogers K, Anantpadma M, Singh BK, Sakurai Y, Bair T, Miller-Hunt C, Sinn P, Davey RA, Monick MM, Maury W. 2015. Interferon-gamma inhibits Ebola virus infection. *PLoS Pathog* 11: e1005263. <https://doi.org/10.1371/journal.ppat.1005263>.
- Barkhouse DA, Garcia SA, Bongiorno EK, Lebrun A, Faber M, Hooper DC. 2015. Expression of interferon gamma by a recombinant rabies virus strongly attenuates the pathogenicity of the virus via induction of type I interferon. *J Virol* 89:312–322. <https://doi.org/10.1128/JVI.01572-14>.
- Iversen MB, Paludan SR. 2010. Mechanisms of type III interferon expression. *J Interferon Cytokine Res* 30:573–578. <https://doi.org/10.1089/jir.2010.0063>.
- Wei H, Wang S, Chen Q, Chen Y, Chi X, Zhang L, Huang S, Gao GF, Chen JL. 2014. Suppression of interferon lambda signaling by SOCS-1 results in their excessive production during influenza virus infection. *PLoS Pathog* 10:e1003845. <https://doi.org/10.1371/journal.ppat.1003845>.
- Sommereyns C, Paul S, Staeheli P, Michiels T. 2008. IFN-lambda (IFN-lambda) is expressed in a tissue-dependent fashion and primarily acts on epithelial cells in vivo. *PLoS Pathog* 4:e1000017. <https://doi.org/10.1371/journal.ppat.1000017>.
- Dunham EC, Banadyga L, Groseth A, Chiramel AI, Best SM, Ebihara H, Feldmann H, Hoenen T. 2015. Assessing the contribution of interferon antagonism to the virulence of West African Ebola viruses. *Nat Commun* 6:8000. <https://doi.org/10.1038/ncomms9000>.
- Kuhn JH. 2008. *Filoviruses*, 1st ed. Springer, New York, NY.
- Ilinykh PA, Lubaki NM, Widen SG, Renn LA, Theisen TC, Rabin RL, Wood TG, Bukreyev A. 2015. Different temporal effects of Ebola virus VP35 and VP24 proteins on global gene expression in human dendritic cells. *J Virol* 89:7567–7583. <https://doi.org/10.1128/JVI.00924-15>.
- Lubaki NM, Ilinykh P, Pietzsch C, Tigabu B, Freiberg AN, Koup RA, Bukreyev A. 2013. The lack of maturation of Ebola virus-infected den-

- dratic cells results from the cooperative effect of at least two viral domains. *J Virol* 87:7471–7485. <https://doi.org/10.1128/JVI.03316-12>.
17. Prins KC, Delpeut S, Leung DW, Reynard O, Volchkova VA, Reid SP, Ramanan P, Cardenas WB, Amarasinghe GK, Volchkov VE, Basler CF. 2010. Mutations abrogating VP35 interaction with double-stranded RNA render Ebola virus avirulent in guinea pigs. *J Virol* 84:3004–3015. <https://doi.org/10.1128/JVI.02459-09>.
 18. Albarino CG, Wiggleton Guerrero L, Spengler JR, Uebelhoer LS, Chakrabarti AK, Nichol ST, Towner JS. 2015. Recombinant Marburg viruses containing mutations in the IID region of VP35 prevent inhibition of host immune responses. *Virology* 476:85–91. <https://doi.org/10.1016/j.virol.2014.12.002>.
 19. Hartman AL, Dover JE, Towner JS, Nichol ST. 2006. Reverse genetic generation of recombinant Zaire Ebola viruses containing disrupted IRF-3 inhibitory domains results in attenuated virus growth in vitro and higher levels of IRF-3 activation without inhibiting viral transcription or replication. *J Virol* 80:6430–6440. <https://doi.org/10.1128/JVI.00044-06>.
 20. Lubaki NM, Younan P, Santos RI, Meyer M, Iampietro M, Koup RA, Bukreyev A. 2016. The Ebola interferon inhibiting domains attenuate and dysregulate cell-mediated immune responses. *PLoS Pathog* 12:e1006031. <https://doi.org/10.1371/journal.ppat.1006031>.
 21. Mateo M, Reid SP, Leung LW, Basler CF, Volchkov VE. 2010. Ebolavirus VP24 binding to karyopherins is required for inhibition of interferon signaling. *J Virol* 84:1169–1175. <https://doi.org/10.1128/JVI.01372-09>.
 22. Valmas C, Grosch MN, Schumann M, Olejnik J, Martinez O, Best SM, Krahling V, Basler CF, Muhlberger E. 2010. Marburg virus evades interferon responses by a mechanism distinct from Ebola virus. *PLoS Pathog* 6:e1000721. <https://doi.org/10.1371/journal.ppat.1000721>.
 23. Luis AD, Hayman DT, O'Shea TJ, Cryan PM, Gilbert AT, Pulliam JR, Mills JN, Timonin ME, Willis CK, Cunningham AA, Fooks AR, Rupprecht CE, Wood JL, Webb CT. 2013. A comparison of bats and rodents as reservoirs of zoonotic viruses: are bats special? *Proc Biol Sci* 280:20122753. <https://doi.org/10.1098/rspb.2012.2753>.
 24. Leroy EM, Kumulungui B, Pourrut X, Rouquet P, Hassanin A, Yaba P, Delicat A, Paweska JT, Gonzalez JP, Swanepoel R. 2005. Fruit bats as reservoirs of Ebola virus. *Nature* 438:575–576. <https://doi.org/10.1038/438575a>.
 25. Towner JS, Pourrut X, Albarino CG, Nkogue CN, Bird BH, Grard G, Ksiazek TG, Gonzalez JP, Nichol ST, Leroy EM. 2007. Marburg virus infection detected in a common African bat. *PLoS One* 2:e764. <https://doi.org/10.1371/journal.pone.0000764>.
 26. Towner JS, Amman BR, Sealy TK, Carroll SA, Comer JA, Swanepoel R, Paddock CD, Balinandi S, Khristova ML, Formenty PB, Albarino CG, Miller DM, Reed ZD, Kayiwa JT, Mills JN, Cannon DL, Greer PW, Byaruhanga E, Farnon EC, Atimnedi P, Okware S, Katongole-Mbidde E, Downing R, Tappero JW, Zaki SR, Ksiazek TG, Nichol ST, Rollin PE. 2009. Isolation of genetically diverse Marburg viruses from Egyptian fruit bats. *PLoS Pathog* 5:e1000536. <https://doi.org/10.1371/journal.ppat.1000536>.
 27. Olival KJ, Hayman DT. 2014. Filoviruses in bats: current knowledge and future directions. *Viruses* 6:1759–1788. <https://doi.org/10.3390/v6041759>.
 28. Swanepoel R, Leman PA, Burt FJ, Zachariades NA, Braack LE, Ksiazek TG, Rollin PE, Zaki SR, Peters CJ. 1996. Experimental inoculation of plants and animals with Ebola virus. *Emerg Infect Dis* 2:321–325. <https://doi.org/10.3201/eid0204.960407>.
 29. Paweska JT, Storm N, Grobbelaar AA, Markotter W, Kemp A, Jansen van Vuren P. 2016. Experimental inoculation of Egyptian fruit bats (*Rousettus aegyptiacus*) with Ebola virus. *Viruses* 8:29. <https://doi.org/10.3390/v8020029>.
 30. Paweska JT, Jansen van Vuren P, Fenton KA, Graves K, Grobbelaar AA, Moolla N, Leman P, Weyer J, Storm N, McCulloch SD, Scott TP, Markotter W, Odendaal L, Clift SJ, Geisbert TW, Hale MJ, Kemp A. 2015. Lack of Marburg virus transmission from experimentally infected to susceptible in-contact Egyptian fruit bats. *J Infect Dis* 212(Suppl 2):S109–S118. <https://doi.org/10.1093/infdis/jiv132>.
 31. Paweska JT, Jansen van Vuren P, Masumu J, Leman PA, Grobbelaar AA, Birkhead M, Clift S, Swanepoel R, Kemp A. 2012. Virological and serological findings in *Rousettus aegyptiacus* experimentally inoculated with Vero cells-adapted Hogan strain of Marburg virus. *PLoS One* 7:e45479. <https://doi.org/10.1371/journal.pone.0045479>.
 32. Amman BR, Jones ME, Sealy TK, Uebelhoer LS, Schuh AJ, Bird BH, Coleman-McCray JD, Martin BE, Nichol ST, Towner JS. 2015. Oral shedding of Marburg virus in experimentally infected Egyptian fruit bats (*Rousettus aegyptiacus*). *J Wildl Dis* 51:113–124. <https://doi.org/10.7589/2014-08-198>.
 33. Middleton DJ, Morrissy CJ, van der Heide BM, Russell GM, Braun MA, Westbury HA, Halpin K, Daniels PW. 2007. Experimental Nipah virus infection in pteropid bats (*Pteropus poliocephalus*). *J Comp Pathol* 136:266–272. <https://doi.org/10.1016/j.jcpa.2007.03.002>.
 34. Schountz T. 2014. Immunology of bats and their viruses: challenges and opportunities. *Viruses* 6:4880–4901. <https://doi.org/10.3390/v6124880>.
 35. Baker ML, Zhou P. 2015. Bat immunology, p 327–348. In Wang L-F, Cowled C (ed), *Bats and viruses: a new frontier of emerging infectious diseases*. John Wiley & Sons, New York, NY.
 36. Jones ME, Schuh AJ, Amman BR, Sealy TK, Zaki SR, Nichol ST, Towner JS. 2015. Experimental inoculation of Egyptian rousette bats (*Rousettus aegyptiacus*) with viruses of the Ebolavirus and Marburgvirus genera. *Viruses* 7:3420–3442. <https://doi.org/10.3390/v7072779>.
 37. Ling PD, Warren MK, Vogel SN. 1985. Antagonistic effect of interferon-beta on the interferon-gamma-induced expression of Ia antigen in murine macrophages. *J Immunol* 135:1857–1863.
 38. Taniguchi T, Takaoka A. 2001. A weak signal for strong responses: interferon-alpha/beta revisited. *Nat Rev Mol Cell Biol* 2:378–386. <https://doi.org/10.1038/35073080>.
 39. Towner JS, Paragas J, Dover JE, Gupta M, Goldsmith CS, Huggins JW, Nichol ST. 2005. Generation of eGFP expressing recombinant Zaire ebolavirus for analysis of early pathogenesis events and high-throughput antiviral drug screening. *Virology* 332:20–27. <https://doi.org/10.1016/j.virol.2004.10.048>.
 40. Park MS, Shaw ML, Munoz-Jordan J, Cros JF, Nakaya T, Bouvier N, Palese P, Garcia-Sastre A, Basler CF. 2003. Newcastle disease virus (NDV)-based assay demonstrates interferon-antagonist activity for the NDV V protein and the Nipah virus V, W, and C proteins. *J Virol* 77:1501–1511. <https://doi.org/10.1128/JVI.77.2.1501-1511.2003>.
 41. Zhou P, Cowled C, Mansell A, Monaghan P, Green D, Wu L, Shi Z, Wang LF, Baker ML. 2014. IRF7 in the Australian black flying fox, *Pteropus alecto*: evidence for a unique expression pattern and functional conservation. *PLoS One* 9:e103875. <https://doi.org/10.1371/journal.pone.0103875>.
 42. Zhou P, Cowled C, Todd S, Crameri G, Virtue ER, Marsh GA, Klein R, Shi Z, Wang LF, Baker ML. 2011. Type III IFNs in pteropid bats: differential expression patterns provide evidence for distinct roles in antiviral immunity. *J Immunol* 186:3138–3147. <https://doi.org/10.4049/jimmunol.1003115>.
 43. Zhang G, Cowled C, Shi Z, Huang Z, Bishop-Lilly KA, Fang X, Wynne JW, Xiong Z, Baker ML, Zhao W, Tachedjian M, Zhu Y, Zhou P, Jiang X, Ng J, Yang L, Wu L, Xiao J, Feng Y, Chen Y, Sun X, Zhang Y, Marsh GA, Crameri G, Broder CC, Frey KG, Wang LF, Wang J. 2013. Comparative analysis of bat genomes provides insight into the evolution of flight and immunity. *Science* 339:456–460. <https://doi.org/10.1126/science.1230835>.
 44. Baker ML, Schountz T, Wang LF. 2013. Antiviral immune responses of bats: a review. *Zoonoses Public Health* 60:104–116. <https://doi.org/10.1111/j.1863-2378.2012.01528.x>.
 45. Zhou P, Tachedjian M, Wynne JW, Boyd V, Cui J, Smith I, Cowled C, Ng JH, Mok L, Michalski WP, Mendenhall IH, Tachedjian G, Wang LF, Baker ML. 2016. Contraction of the type I IFN locus and unusual constitutive expression of IFN-alpha in bats. *Proc Natl Acad Sci U S A* 113:2696–2701. <https://doi.org/10.1073/pnas.1518240113>.
 46. Geisbert TW, Hensley LE, Larsen T, Young HA, Reed DS, Geisbert JB, Scott DP, Kagan E, Jahrling PB, Davis KJ. 2003. Pathogenesis of Ebola hemorrhagic fever in cynomolgus macaques: evidence that dendritic cells are early and sustained targets of infection. *Am J Pathol* 163:2347–2370. [https://doi.org/10.1016/S0002-9440\(10\)63591-2](https://doi.org/10.1016/S0002-9440(10)63591-2).
 47. Kepler TB, Sample C, Hudak K, Roach J, Haines A, Walsh A, Ramsburg EA. 2010. Chiropteran types I and II interferon genes inferred from genome sequencing traces by a statistical gene-family assembler. *BMC Genomics* 11:444. <https://doi.org/10.1186/1471-2164-11-444>.
 48. He G, He B, Racey PA, Cui J. 2010. Positive selection of the bat interferon alpha gene family. *Biochem Genet* 48:840–846. <https://doi.org/10.1007/s10528-010-9365-9>.
 49. Feagins AR, Basler CF. 2015. Lloviu virus VP24 and VP35 proteins function as innate immune antagonists in human and bat cells. *Virology* 485:145–152. <https://doi.org/10.1016/j.virol.2015.07.010>.
 50. Streicker DG, Turmelle AS, Vonhof MJ, Kuzmin IV, McCracken GF, Rupprecht CE. 2010. Host phylogeny constrains cross-species emergence and establishment of rabies virus in bats. *Science* 329:676–679. <https://doi.org/10.1126/science.1188836>.
 51. Mortlock M, Kuzmin IV, Weyer J, Gilbert AT, Agwanda B, Rupprecht CE,

- Nel LH, Kearney T, Malekani JM, Markotter W. 2015. Novel paramyxoviruses in bats from sub-Saharan Africa, 2007-2012. *Emerg Infect Dis* 21:1840–1843. <https://doi.org/10.3201/eid2110.140368>.
52. Holzer M, Kraehling V, Amman F, Barth E, Bernhart SH, Carmelo VA, Collatz M, Doose G, Eggenhofer F, Ewald J, Fallmann J, Feldhahn LM, Fricke M, Gebauer J, Gruber AJ, Hufsky F, Indrischek H, Kanton S, Linde J, Mostajo N, Ochsenreiter R, Riege K, Rivarola-Duarte L, Sahyoun AH, Saunders SJ, Seemann SE, Tanzer A, Vogel B, Wehner S, Wolfinger MT, Backofen R, Gorodkin J, Grosse I, Hofacker I, Hoffmann S, Kaleta C, Stadler PF, Becker S, Marz M. 2016. Differential transcriptional responses to Ebola and Marburg virus infection in bat and human cells. *Sci Rep* 6:34589. <https://doi.org/10.1038/srep34589>.
 53. Matsumoto M, Tanaka N, Harada H, Kimura T, Yokochi T, Kitagawa M, Schindler C, Taniguchi T. 1999. Activation of the transcription factor ISGF3 by interferon-gamma. *Biol Chem* 380:699–703.
 54. Levy DE, Lew DJ, Decker T, Kessler DS, Darnell JE, Jr. 1990. Synergistic interaction between interferon-alpha and interferon-gamma through induced synthesis of one subunit of the transcription factor ISGF3. *EMBO J* 9:1105–1111.
 55. Sheppard P, Kindsvogel W, Xu W, Henderson K, Schlutsmeyer S, Whitmore TE, Kuestner R, Garrigues U, Birks C, Roraback J, Ostrand C, Dong D, Shin J, Presnell S, Fox B, Haldeman B, Cooper E, Taft D, Gilbert T, Grant FJ, Tackett M, Krivan W, McKnight G, Clegg C, Foster D, Klucher KM. 2003. IL-28, IL-29 and their class II cytokine receptor IL-28R. *Nat Immunol* 4:63–68. <https://doi.org/10.1038/ni873>.
 56. Kotenko SV, Gallagher G, Baurin VV, Lewis-Antes A, Shen M, Shah NK, Langer JA, Sheikh F, Dickensheets H, Donnelly RP. 2003. IFN-lambdas mediate antiviral protection through a distinct class II cytokine receptor complex. *Nat Immunol* 4:69–77. <https://doi.org/10.1038/ni875>.
 57. Kotenko SV. 2011. IFN-lambdas. *Curr Opin Immunol* 23:583–590. <https://doi.org/10.1016/j.coi.2011.07.007>.
 58. Jordan I, Horn D, Oehmke S, Leendertz FH, Sandig V. 2009. Cell lines from the Egyptian fruit bat are permissive for modified vaccinia Ankara. *Virus Res* 145:54–62. <https://doi.org/10.1016/j.virusres.2009.06.007>.
 59. Kuhl A, Hoffmann M, Muller MA, Munster VJ, Gnirss K, Kiene M, Tsegaye TS, Behrens G, Herrler G, Feldmann H, Drosten C, Pohlmann S. 2011. Comparative analysis of Ebola virus glycoprotein interactions with human and bat cells. *J Infect Dis* 204(Suppl 3):S840–S849. <https://doi.org/10.1093/infdis/jir306>.
 60. Shaw G, Morse S, Ararat M, Graham FL. 2002. Preferential transformation of human neuronal cells by human adenoviruses and the origin of HEK 293 cells. *FASEB J* 16:869–871.
 61. Bwaka MA, Bonnet MJ, Calain P, Colebunders R, De Roo A, Guimard Y, Katwiri KR, Kibadi K, Kipasa MA, Kuvula KJ, Mapanda BB, Massamba M, Mupapa KD, Muyembe-Tamfum JJ, Ndaberey E, Peters CJ, Rollin PE, Van den Enden E, Van den Enden E. 1999. Ebola hemorrhagic fever in Kikwit, Democratic Republic of the Congo: clinical observations in 103 patients. *J Infect Dis* 179(Suppl 1):S1–S7. <https://doi.org/10.1086/514308>.
 62. Baize S, Pannetier D, Oestereich L, Rieger T, Koivogui L, Magassouba N, Soropogui B, Sow MS, Keita S, De Clerck H, Tiffany A, Dominguez G, Loua M, Traore A, Kolie M, Malano ER, Heleze E, Bocquin A, Mely S, Raoul H, Caro V, Cadar D, Gabriel M, Pahlmann M, Tappe D, Schmidt-Chanasit J, Impouma B, Diallo AK, Formenty P, Van Herp M, Gunther S. 2014. Emergence of Zaire Ebola virus disease in Guinea. *N Engl J Med* 371:1418–1425. <https://doi.org/10.1056/NEJMoa1404505>.
 63. Albarino CG, Uebelhoer LS, Vincent JP, Khristova ML, Chakrabarti AK, McElroy A, Nichol ST, Towner JS. 2013. Development of a reverse genetics system to generate recombinant Marburg virus derived from a bat isolate. *Virology* 446:230–237. <https://doi.org/10.1016/j.virol.2013.07.038>.
 64. Towner JS, Khristova ML, Sealy TK, Vincent MJ, Erickson BR, Bawiec DA, Hartman AL, Comer JA, Zaki SR, Ströher U, Gomes da Silva F, del Castillo F, Rollin PE, Ksiazek TG, Nichol ST. 2006. Marburgvirus genomics and association with a large hemorrhagic fever outbreak in Angola. *J Virol* 80:6497–6516. <https://doi.org/10.1128/JVI.00069-06>.
 65. Lee AK, Kulcsar KA, Elliott O, Khiabani H, Nagle ER, Jones ME, Amman BR, Sanchez-Lockhart M, Towner JS, Palacios G, Rabadan R. 2015. De novo transcriptome reconstruction and annotation of the Egyptian rousette bat. *BMC Genomics* 16:1033. <https://doi.org/10.1186/s12864-015-2124-x>.
 66. Pfaffl MW, Horgan GW, Dempfle L. 2002. Relative expression software tool (REST) for group-wise comparison and statistical analysis of relative expression results in real-time PCR. *Nucleic Acids Res* 30:e36. <https://doi.org/10.1093/nar/30.9.e36>.